

*Linking Riparian Flow-Concentration Integration Modeling and HSPF  
to Predict Background Methylmercury Concentrations in Northeastern  
Minnesota Streams*

A Thesis  
SUBMITTED TO THE FACULTY OF  
UNIVERSITY OF MINNESOTA  
BY

*Joseph Wes Rutelonis*

IN PARTIAL FULFILLMENT OF THE REQUIREMENTS  
FOR THE DEGREE OF  
MASTER OF SCIENCE

David L. Fox, Michael E. Berndt

May 2017



## **Acknowledgements**

This study was funded by the Minnesota Department of Natural Resources Clean Water, Iron Ore Cooperative Research, and Cooperative Environmental Research Funds. I wish to thank: Dr. Jon Butcher and his team at TetraTech for HSPF model development, for important guidance in HSPF model use and in general for being very easy a pleasure to work with, Dr. Chuck Regan of the Minnesota Pollution Control Agency for HSPF guidance, advice and for offering perspective pertaining to the world of watershed modeling, Dr. Bruce Monson of the Minnesota Pollution Control Agency for supervising data collection efforts, assisting in FLUX regression modeling and providing important comments and Drs. Gene-Hua Crystal Ng and Nathan Johnson at the University of Minnesota for general guidance, for teaching me how to make/use models and for providing important comments.

## Dedication

First and foremost, I would like to thank Dr. Michael E. Berndt. You have, over the last four years, been essential to my professional development and survival in general. When I first moved to Minnesota from Oklahoma, I didn't know a soul in this strange land where the people talk funny and they care about water, among other things, and I was in desperate need of a job. After begging a little (pestering really) and even offering to volunteer, Mike offered me that job sampling river water in iron ore country... and when that job had ended he helped find me another job... and when that job had ended he helped me develop the idea and find funding for the thesis you are about to read. Mike, your support has meant the world to me and I am proud to call you my mentor and friend. Thank you.

To Dr. David L. Fox, thank you for your endless advice, for your laid back advising style and for the mountain of baby items and parenting advice that you donated to our cause. This work literally could not have been accomplished without you. Thank you very much.

To my Mother and Father In-law, Bob and Kathy Junghans, thank you so much for your help, guidance, support, soup and enthusiasm for letting my family terrorize your home. Without the constant love and support of those around me, this work and all my life's endeavors would not be possible. Thank you.

To my brother Grayson and sister Lamarie, I would achieve very little without your positive influence. You guys are amazing at life and two of my best friends and role-models. Thank you for teaching me, leading me in the right direction (in a round-about sort of way, of course), and loving me when very few people would even dream of it. I love you both.

To my folks, Tonja and Joe Rutelonis, mom and dad, Tonisha and Joe Daety (pronunciation: jō dāədē), I love you and I appreciate you more than you will ever know. Thank you for encouraging me to explore my surroundings and develop a deep seated appreciation for the natural world. Thank you for never skipping a roadside "geologic point

of interest” or an interesting outcrop worth climbing up to. Thank you for being my defenders and my protectors. I owe you a lot. You guys win parenting for sure, you’re real good, and I love you.

Finally, and most importantly, this thesis is dedicated to my inexplicably caring, wildly intelligent, incessantly patient and astonishingly beautiful wife, Ashley. You inspire me to be a better father, husband and person and... *you put up with me* and for those reasons, my appreciation for you cannot be overstated. I love you so very much. To my precious son Werner, you came into my life mid-graduate school and I wouldn’t have had it any other way. The vast majority of this thesis was written in Southeastern Minnesota farm country with you, a newborn at the time, by my side armed with an arsenal of seemingly unending and adorable distractions. I am unbelievably proud of you and can’t wait to teach you about geology. To my three trouble making dogs, Marley, Macy and Winston, I dedicate nothing. You guys are the worst. No, but really, you guys are passionate and crazy and you make my life exciting like no one else ever could; I love you. You five believe in me, bring me joy and happiness, love me unconditionally, and are essential to my life and accomplishments.

Ps. To all who interacted with me during my time as a graduate student, sorry for the odd smells and thank you for discussing hydrology and watershed modeling more than you ever wanted/willingly agreed to.

## **Abstract**

The St. Louis River Watershed in Northeastern Minnesota has been studied extensively to determine the degree to which sulfate loading from the Mesabi Iron Range affects microbial methylation and bioaccumulation of mercury. Recent studies have identified natural processes unrelated to mining, most often in non-mining portions of the region, as the primary source of methylmercury loading to the river. Here, we further evaluate those contributions by interpreting water chemistry (DOC, THg, MeHg and Fe) from seven St. Louis River tributaries and three main channel sampling sites with the Riparian Flow-Concentration Integration Model (RIM) which was developed for interpretation of stream chemistry in boreal streams in Sweden. This model assumes that riparian wetland soil, the last substrate that porewater encounters before becoming river water, controls the chemistry of local groundwater recharging the river. In locations that contain mixed mining and non-mining contributions, a watershed model (Hydrologic Simulation Program – Fortran: HSPF) was used to estimate the relative groundwater and point source contributions. The RIM approach with soil temperature incorporated as a time-varying parameter is more physically based compared to regression-based methods that have been used previously to interpret stream loads in the region. The comparison of Nash-Sutcliffe model efficiency calculations for both RIM and regression-based models indicate that RIM offers a significant improvement in model predictive power. Since stream flow and temperature are the main drivers, RIM reduces the necessity for widespread, repetitive methylmercury sampling efforts to estimate methylmercury loads.

## Table of Contents

Abstract.....	iv
List of Tables .....	vi
List of Figures .....	vii
List of Appendices .....	viii
Introduction.....	1
Site Descriptions .....	6
Methods – Model Descriptions.....	8
Hydrologic Simulation Program – Fortran (HSPF).....	8
Riparian Flow-Concentration Integration Model (RIM) .....	11
RIM Parameter Estimation .....	15
RIM Uncertainty Analysis .....	16
Results.....	17
Discussion.....	20
Conclusions.....	27
References.....	29

## List of Tables

Table 1 .....	16
Table 2 .....	19

## List of Figures

Figure 1 .....	4
Figure 2 .....	7
Figure 3 .....	10
Figure 4 .....	12
Figure 5 .....	23

## List of Appendices

Appendix 1.....	34
Appendix 2.....	45

## **Introduction**

Mercury (Hg) contamination in fish tissue is pervasive in Minnesota, occurring in lakes and rivers in nearly all watersheds throughout the state (MPCA, 2007). Deposition of Hg in wet and dry form is sourced from global and local atmospheric pools and is derived from both natural and historically elevated anthropogenic sources (Swain, 1992, Engstrom and Swain, 1997, Schroeder et al., 1998). Hg deposition is expected to decrease over time with on-going worldwide efforts to reduce industrial emissions, and this should lead to decreases in mercury levels in fish and aquatic invertebrates (Munthe et al., 2007, MPCA, 2007). However, Hg inventories that have built up in soils over time across the US result in continued contamination in aquatic food webs that may persist for years to decades after the global sources have been decreased (Meili et al., 2003, Atkeson et al., 2003, MPCA, 2007).

Methylmercury (MeHg), the primary organic form of Hg, has far greater bioaccumulative potential than inorganic Hg, and its appearance in terrestrial and aquatic ecosystems is the result of microbial methylation, often linked to sulfate reduction in anaerobic soils (Engstrom, 2007, Compeau and Bartha, 1985, Mason et al., 2005, Benoit, 1999, Gilmour et al., 1992). However, specific gene clusters related to the Hg methylation process have been found recently in a variety of microbial communities, including iron-reducers, methanogens, and others (Parks et al., 2013), having evolved possibly as a general mechanism to detoxify their environment by exuding Hg through the cell

membrane in mobile organic forms (Poulain and Barkay, 2013). While the exact source and cause of methylation may be site dependent, what is clear is that once present, MeHg readily combines with organic thiol groups (organosulfur compounds) and becomes concentrated in living organisms, biomagnifying progressively with trophic level (Skyllberg and Drott, 2010, Skyllberg, 2008, Watras et al., 1998, Rolfhus et al., 2011). Highest tissue concentrations typically occur in the upper levels of aquatic food chains (predatory fish, piscivorous birds, and humans who consume large predatory fish) (MPCA, 2007).

Understanding mercury cycles has become important in the St. Louis River (SLR) Watershed in northern Minnesota, which hosts a globally significant iron ore mining district (Mesabi Iron Range) and extensive economically viable copper-nickel sulfide deposits that currently remain unmined. Those deposits are situated in a relatively rural forested and wetland-rich region known to contain elevated MeHg in fish (MPCA, 2007). Mining can expose rocks containing sulfide minerals to both oxygen and mobile water, resulting in the generation and release of sulfate into nearby lakes, streams and groundwater. Significant positive correlations between non-point source sulfate introduced to wetlands from simulated atmospheric sources and increased net methylation has been demonstrated in northern Minnesota peatlands (Coleman Wasik et al., 2012, Jeremiason et al., 2006), and many studies conducted at local to regional scales have examined the relationship between mine-related sulfate elevations and MeHg production and transport (Bailey et al., 2014a, Bailey et al., 2014b, Berndt et al., 2014, Johnson et al., 2016, Berndt and Bavin, 2012, Jeremiason et al., 2016, Berndt and Bavin, 2009, Berndt and Bavin,

2011). Berndt and Bavin (2012) found that DOC and MeHg in tributaries and the main stem of the St. Louis River all increased and decreased together and suggested that wetlands located primarily in non-mining portions of the watersheds were the dominant sources for both. However, it is unclear whether export of MeHg from wetlands connected to rivers can by itself explain the elevations of MeHg under all flow conditions. It is likely that local groundwater influx through stream-adjacent riparian wetlands plays a major role (Bradley et al., 2012). Berndt et al. (2016) recently compared the chemistry of water collected upstream and downstream from the mining region with output from a watershed model (HSPF) that tracks different sources of water throughout the watershed. They identified summer groundwater recharge, likely flowing through riparian wetland zones throughout the watershed, as the overwhelmingly dominant source of MeHg to the SLR and found that point sources with elevated sulfate from mines add little methylation opportunity to the already high background MeHg found in sulfate impacted streams.

Riparian zones are “vegetated ecosystems along a water body through which energy, materials and water pass” (US EPA), and contain both the chemical constituents and the reducing conditions needed to promote MeHg production and transport to streams (Bishop et al., 2004). In situations where shallow groundwater enters gaining streams or wetlands, porewater derives much of its chemistry from riparian soils immediately adjacent to the stream just prior to entering the surface water flow environment (Bishop et al., 2004). The Riparian Flow-Concentration Integration Model (RIM), which is based on this principle, was developed and used successfully to explain variation in stream water fluxes of dissolved organic carbon (DOC), MeHg and total Hg (THg) in several intensely sampled

streams in boreal regions of Sweden (Eklöf et al., 2015, Winterdahl et al., 2011, Seibert et al., 2009). The geographical setting in Sweden, where the RIM model was developed, is similar to that in northeastern Minnesota as both regions lie in the southern fringe of boreal forest where gaining streams often transect glaciated terrain. While the latitudes of the two regions vary by about 15 degrees, average monthly precipitation and temperature ranges are fairly similar with northern Minnesota having slightly more summer rainfall on an annual basis (Figure 1). THg, MeHg, DOC, and Fe concentration ranges are also similar and respond to seasonal changes in rainfall and streamflow in a comparable manner (Ledesma et al., 2016, Eklöf et al., 2015, Winterdahl et al., 2011, Winterdahl et al., 2014, Berndt et al., 2016). Thus, RIM may provide a method to link stream chemistry to flow in northern Minnesota streams.

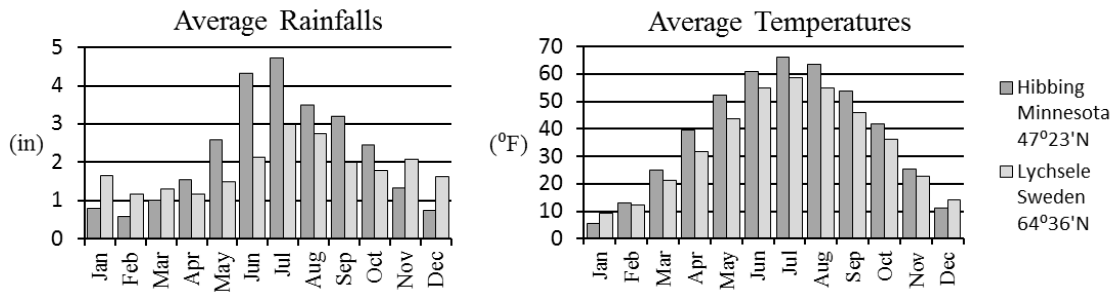


**Figure 1.** Comparison of monthly average temperature and rainfall in boreal (Lychsele, Sweden) and sub-boreal (Hibbing, Minnesota) cities. Both cities are non-coastal, relatively rural and surrounded by lakes. Lychsele and Hibbing were selected for climate comparison based on proximity to past RIM studies and central location on the SLR Watershed, respectively.

Unlike the Swedish systems modeled with RIM, the SLR has mine water that flows directly into or is pumped into some tributary streams that can form a significant portion of total streamflow during winter and late summer dry periods (Berndt et al., 2016). Thus,

a straightforward application of the RIM model would not suffice for Minnesota's mining region. Here, Hydrologic Simulation Program – Fortran (HSPF) was used to help characterize the percentages of total streamflow that comprised groundwater recharge as compared to other sources that can include surface runoff, interlayer flow, or mining/non-mining point source discharges. Although sources other than groundwater are typically small in most parts of the region (Berndt et al., 2016), knowing their magnitude and how they change with time is important. Moreover, because DOC and MeHg are subject to both biotic and abiotic degradation in the water column (Jeremiason et al., 2014b, Jeremiason et al., 2015), HSPF can also be used to provide contextual transit time information at each of the study sites. Combining RIM and HSPF models provides a potential means to estimate chemistry and loading through time for a variety of chemicals that change rapidly in response to both flow and temperature, especially during the summer warm periods.

The current study tests RIM modeling in the St. Louis River and its tributaries using available climate and stream chemistry data and associated flow measurements that were collected in 2012 and 2013. Of significance is whether the method offers an improvement in predictive power compared to more traditional regression-based models typically used to estimate constituent loads in the region. The basic approach of regression-based load calculation uses purely empirical flow/concentration relationships developed from the sample record to interpolate concentrations for an entire flow record. These relationships often rely on flow only and omit important physical parameters such as temperature, thereby providing little insight on the hydrologic and chemical processes that control mercury loading in rivers like the SLR.

## Site Descriptions

The SLR takes a counter-clockwise, semicircular path 180 miles in length through northeast Minnesota draining approximately 9,000 square kilometers and has an overall elevation drop of approximately 335 meters from its uppermost headwaters to its estuary in Lake Superior (Berndt and Bavin, 2012). Hg, MeHg, Fe, and DOC concentrations in the SLR Watershed were studied previously by Berndt and Bavin (2012) at 12 tributaries and three points on the St. Louis River main stem. However, sampling covered mostly a low flow period and most emphasis was placed on chemistry differences between mining and non-mining streams and little to no stream gaging occurred at the majority of sites (Berndt and Bavin, 2012). More recently, Berndt et al. (2016) reported the chemistry of water sampled upstream and downstream from the mining region over a much larger range of hydrologic conditions in 2012 (Berndt et al., 2016). In 2013, 15 water samples were collected from late spring to early fall by the Minnesota Department of Natural Resources at ten sites, and the full chemical measurements were generally accompanied by measurement of stream flow. Sampling points for the tributaries were located just upstream from their confluence with SLR in order to isolate their chemical signal from any mixing with water in the main channel (Figure 2). This study uses only samples that include climate, stream chemistry and flow data in 2012 and 2013 to calibrate the RIM model.

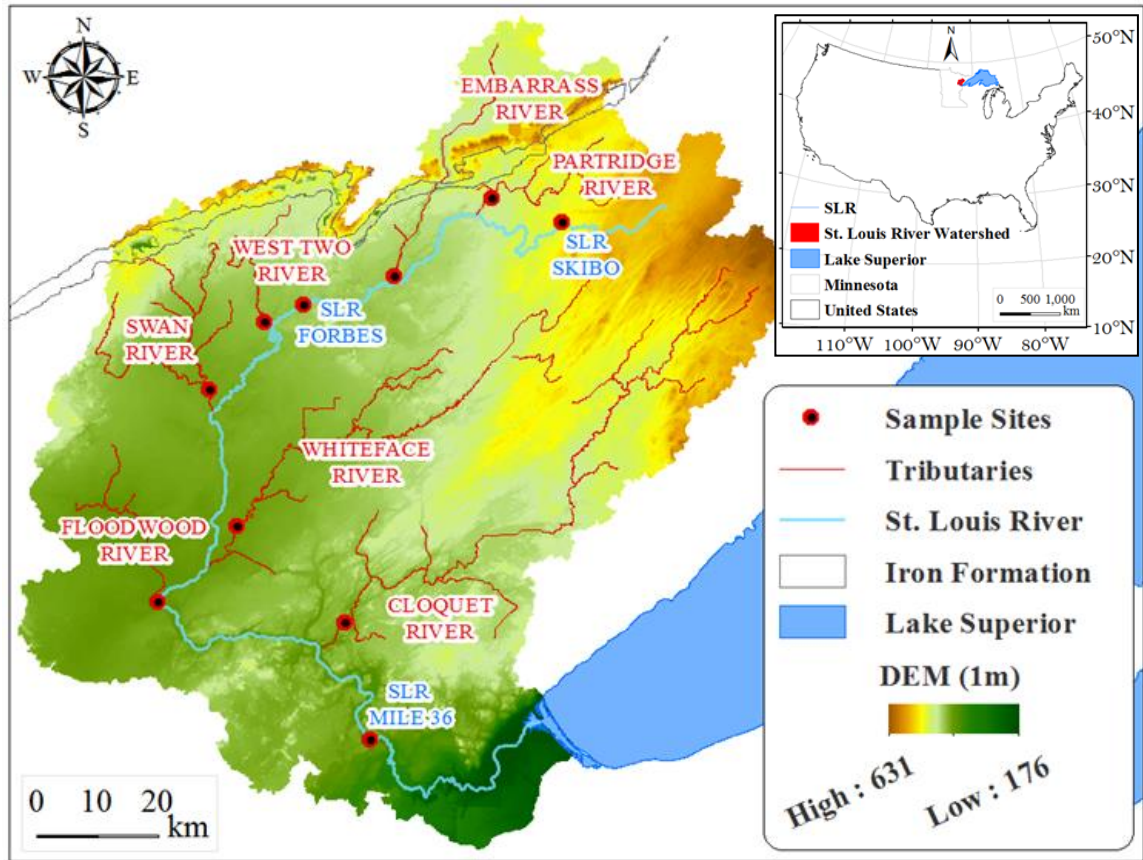


**Figure 2.** Location of the St. Louis River and Cloquet River Watersheds in the United States (right) and the watershed scale map showing 2013 sample locations, tributary names, St. Louis River main channel, Biwabik Iron Formation and a digital elevation model (DEM) for the St. Louis River and Cloquet River drainage areas (left). Labels in blue are SLR sample sites while those in red are tributary sites.

Three of the ten sites were located directly on the SLR main channel. River mile 179 (SLR Skibo) drains an undeveloped region in the northeastern portion of the watershed and is unaffected by any mining, industrial, or municipal inputs. SLR Skibo has been used in previous studies to represent the background characteristics of the watershed (Berndt et al. 2016). SLR river mile 125 (SLR Forbes) and river mile 36 (SLR Scanlon) are downstream from mining inputs and receive mixed water from much larger portions of the

watershed. The Cloquet and Whiteface Rivers are the largest tributaries, and each has large reservoirs in their flow path that potentially impact transit times and chemistry. Each drains approximately 25% of the watershed in a southwesterly direction starting in the northeastern portion of the watershed. The Floodwood and Swan Rivers drain the westernmost portions of the SLR watershed, a region that is relatively flat and largely comprised of forested and non-forested wetlands that are often impacted by extensive agricultural ditching. The West Two, Embarrass and Partridge River confluences make up the remaining sample sites. Each of these rivers drains wetland regions, is impacted by mining and municipal point source discharges, and contain lakes or reservoirs in their flow paths. SLR Skibo and Whiteface, Floodwood, and Cloquet Rivers remain free from mining inputs year-round and are mostly dominated by groundwater inputs with intermittent surface runoff during winter snowmelt and heavy rainfall events. On the other hand, Partridge River, Embarrass River, SLR Forbes, West Two River, Swan River and SLR Scanlon all receive relatively constant mining inputs throughout the year. During wet periods when river water is dominated by natural groundwater recharge, the percentage of mine water is at its lowest values while dry periods tend to yield increasing influence of mining and municipal point source discharges as natural sources diminish (Berndt et al., 2016).

## **Methods – Model Descriptions**

### Hydrologic Simulation Program – Fortran (HSPF)

A HSPF watershed model was used in this study to help characterize the watershed (TetraTech, 2013). A model extension is undergoing calibration and, thus, model output is

used qualitatively to characterize water source and measured flow values are used for fitting chemistry to flow. HSPF is a spatially distributed, soil moisture accounting and surface water flow modeling tool that consists of a series of storage elements (soil, lakes, streams, and snowpack) with user-specified parameterized functions designed to exchange mass and energy between elements (Bicknell et al., 2005). Its lumped domain is also user-defined, usually comprised of sub-watershed divisions or sub-basins each made up of a unique land type composition. HSPF's governing equations are highly parameterized and are designed to facilitate developer calibration to match observed flows through empirically based parameterization methods. Meteorological forcing (precipitation, solar radiation, air temperature, etc.) derived monitoring stations is distributed geographically using Thiessen polygons (TetraTech, 2013). Lake and river volumes and outfall discharges are estimated using bathymetric information from Minnesota state databases. Model developers use this information to generate rating curves for model reaches and reservoirs that determine discharge rates based on stage height.

For the purposes of this study, HSPF was used as a tool to determine the relative contribution of different sources of water throughout the watershed. Different land types cause water to infiltrate at varying rates that, in turn, allocate water to surface runoff, shallow interlayer flow, and active groundwater (groundwater that is hydrologically connected to streams and lakes) in varying proportions. Additionally, water sourced from point sources enters the surface water flow environment independently from the background sources. Computational tracers were applied to each statistically substantial source of water at a constant and equal concentration in order to distinguish and track the

different sources of water throughout their flow path (Berndt et al., 2016). By doing so, at a given sub-basin outfall that coincides with a sampling point, the percentage of the flow volume that is made up of active groundwater can be calculated and used to normalize observed flows to water that has flowed through the subsurface. This facilitates the use of RIM by constraining lateral flux through the riparian zone as equal to streamflow. In practice, the percentage of flow comprised of active groundwater calculated with HSPF was multiplied by observed streamflow in order to estimate the groundwater portion of the flow volume. Source distributions described above can also be compared to water chemistry (Figure 3).

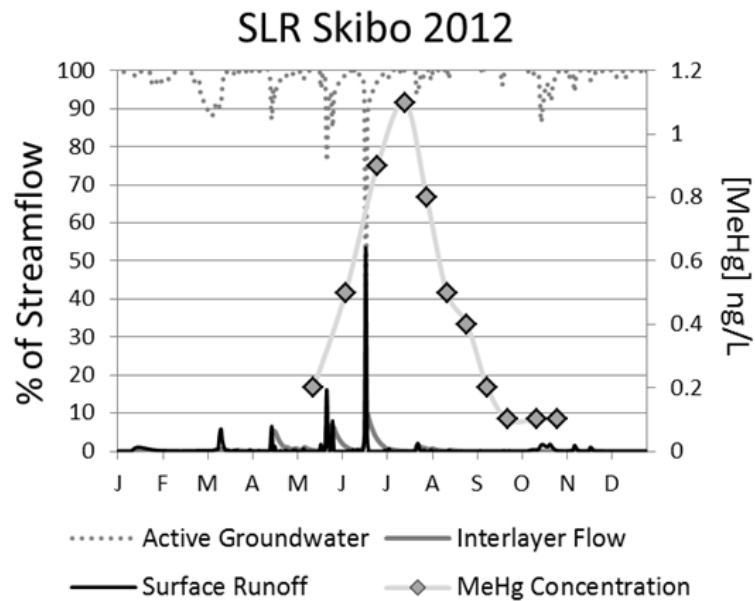


**Figure 3.** Relative distribution of HSPF calculated percent water source (active groundwater, surface runoff, interlayer flow) compared to MeHg concentration in the SLR at the SLR Skibo site through 2012 (x-axis: tick marks are first day of each month labeled using the first letter of each month). Surface runoff and interlayer flow remain a small percentage of the total flow during most of the year except during heavy rainfall events. The river experienced high MeHg concentrations from early June through late August despite the lack of runoff/interlayer contributions indicating that runoff and interlayer flow fluxes do not make up a large portion of the total MeHg load and rather that active groundwater, as expected, controls MeHg loading.

Because some components may degrade or react in the water column, HSPF was also used to approximate transit time information using methods described by Berndt et al. (2016). Briefly, in two separate HSPF model runs, tracers were applied to water as they recharged the rivers throughout the watershed and were allowed to decay in one run but were treated conservatively in the other. By comparing decaying vs. non-decaying tracer concentrations at specific sites, an indication of the average transit time for molecules at that site can be calculated using a first order decay equation similar to radioactive decay ( $-\ln[*C/C]/k$  where  $*C$  and  $C$  are the decaying and non-decaying tracer, respectively;  $k$  is the decay rate). The water at the site contains a mixture of old molecules (those that have been exposed at the surface for a relatively long time) and young molecules (those that entered the flow environment near the sampling site) and is therefore an operationally defined, flow-weighted transit time. In this case the calculated flow-weighted transit times were used to examine the potential effects that reservoirs/storage and stream length may have on stream chemistry and RIM modeling.

#### Riparian Flow-Concentration Integration Model (RIM)

The RIM approach focuses on the riparian zone as the dominant source of chemical constituents during groundwater recharge and assumes that lateral flux and porewater chemistry in the riparian zone vary significantly depending on depth in the z-direction (Seibert et al., 2009) (Figure 4). While transmissivity almost always increases toward the

soil surface, chemistry gradients can increase, decrease or fluctuate with depth depending on the reactions taking place in riparian soils. The RIM approach simultaneously integrates these two relationships providing a means to calculate response of stream chemistry to changing flow conditions.

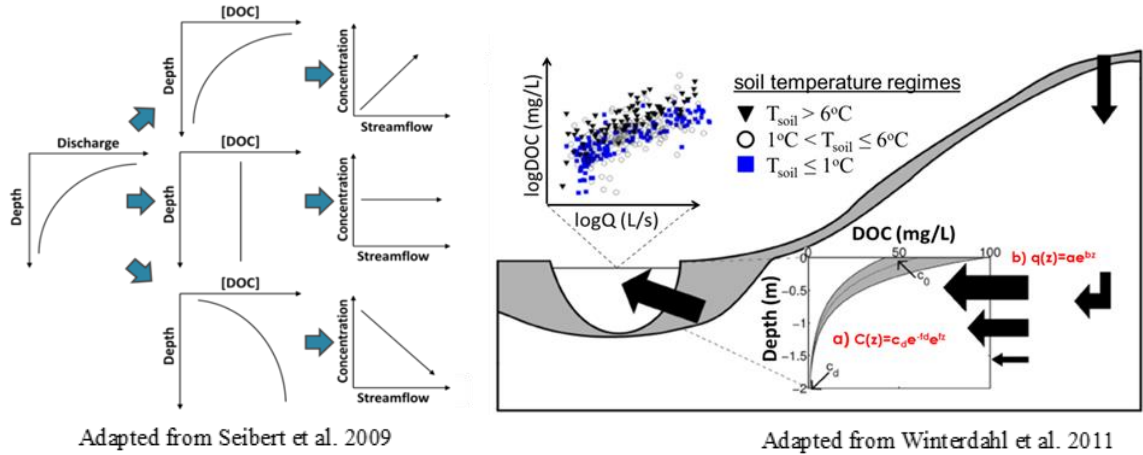


**Figure 4.** Schematic showing generalized relationships between riparian groundwater depth, dissolved organic carbon concentration and total streamflow (left) and hillslope hydrology as it relates to riparian flow-concentration integration (right). The red equations are the pore water concentration profile in the riparian soil (a) and the lateral flow across that profile at different depths in the soil (b). The effect of soil temperature on stream chemistry is evident in the downward shift of DOC stream concentrations seen in the scatter plot.

The flow-concentration integral is the sum, over depth, of lateral water flux,  $q$  [ $\text{L}^2 \text{T}^{-1}$ ], times porewater concentration,  $c$  [ $\text{M L}^{-3}$ ]. The constituent mass load  $L$  [ $\text{M T}^{-1}$ ], as a function of depth  $z$  [ $\text{L}$ ], is the integral of lateral flux,  $q(z)$ , and concentration,  $c(z)$ , from an arbitrary base depth,  $z_B$ , to the elevation of the shallow groundwater table,  $z_{GW}$ . Lateral fluxes below  $z_B$  and above  $z_{GW}$  are assumed to be negligible. Assuming that streamflow,  $Q$  [ $\text{L}^3 \text{T}^{-1}$ ], normalized to groundwater by subtracting off other sources using HSPF, equals the riparian lateral flux integrated over the entire length of the upstream stream network (stream water

is comprised entirely of shallow active groundwater),  $c_{Stream}$  [ $M L^{-3}$ ] can then be calculated by dividing the constituent load integral by the lateral water flux integral:

$$c_{Stream} = \frac{L}{Q} = \frac{\int_{z_B}^{z_{GW}} q(z)c(z)dz}{\int_{z_B}^{z_{GW}} q(z)dz} \quad (1.1)$$

The shape of the depth-dependent lateral water flux and soil chemistry profiles can be defined as exponential functions, with parameters ( $a$ ,  $b$ ,  $c_o$ , and  $f$ ):

$$q(z) = ae^{bz} \quad (2)$$

$$c(z) = c_o e^{fz} \quad (3)$$

with  $z_B$  and  $z_{GW}$  defined above. The constituent mass load can then be calculated as a function of depth to shallow groundwater

$$L = \int_{z_B}^{z_{GW}} ae^{bz}c_o e^{fz} dz \quad (4)$$

where  $a$ ,  $b$  and  $c_o$  can be calculated based on empirical stream observations at low flow conditions and  $f$  remains a free parameter that can be solved for iteratively using a generalized reduced gradient nonlinear solver method in order to fit the model to observed loads. An analytical solution to this equation was developed by Seibert et al. (2009) resulting in the following power law equation:

$$c_{Stream} = c_o \frac{\left(\frac{a}{b}\right)^{1-\eta}}{\eta} Q^{\eta-1} \quad (1.2)$$

$$\eta = \frac{b+f}{b}$$

The concentration profile ( $c(z)=c_0e^{fz}$ ) is defined in this equation under steady-state conditions, whereby the chemical profile does not vary temporally. In reality, riparian soil profiles for constituents like DOC, THg, Fe or MeHg may vary depending on soil temperature and its inherent influence on microbial productivity. Under cooler conditions, microbial activity may be stunted shifting the profile towards lower concentrations while warmer soil temperatures will do the opposite and allow for higher levels of net MeHg and DOC production by microbial communities. In order to incorporate the influence of soil temperature, we have modified the parameters  $c_0$  and  $f$  in the soil concentration profile.

$$c_o(t) = c_o e^{\kappa T_i} \quad (5)$$

$$f(t) = f e^{\lambda T_i} \quad (6)$$

$T_i$  in this case was calculated using a 60-day running mean of local air temperature at a given time step (Winterdahl, et al., 2011) and  $\kappa$  and  $\lambda$  are free parameters describing the effect of temperature on the soil concentration profile. By introducing soil temperature, we have added two new free parameters, leaving a total of four fixed (calculated or observed) parameters ( $a$ ,  $b$ ,  $c_o$  and  $T_i$ ) and three free, adjustable parameters ( $f$ ,  $\kappa$ , and  $\lambda$ ). This leaves us with a modified analytical solution that incorporates the soil temperature proxy.

$$c_{Stream} = c_o(t) \frac{(a/b)^{1-\eta(t)}}{\eta(t)} Q^{\eta(t)-1} \quad (1.3)$$

$$c_{Stream} = c_o e^{\kappa T_i} \frac{(a/b)^{1-\delta}}{\delta} Q^{\delta-1} \quad (1.4)$$

$$\delta = \frac{(b+fe^{\lambda T_i})}{b}$$

### RIM Parameter Estimation

Observed streamflow normalized to the groundwater proportion was used to constrain the lateral flux component of the model. The multiplier of this component,  $a$ , is equal to the minimum observed streamflow,  $Q$ , at each site;  $b$  can then be calculated using a rating curve. The chemistry profile parameters were derived in a similar manner, where  $c_o$  can be assumed to have a consistent value at low-flow,  $c_d$ , at each site

$$c_o = c_d e^{-fz} dz \quad (7)$$

that represents the concentration of the constituent when streamflow was at its lowest observed value. This leaves  $f$  as the only free parameter in the steady-state version of the model.

A 60-day running mean of air-temperature was chosen as a proxy for soil temperature to account for the lag in soil response to changing weather conditions. This method was developed for RIM previously by Winterdahl et al. (2011) and was also used here based on tests revealing better performance than shorter 11-day and 30-day running

means. Having solved for  $a$ ,  $b$ ,  $c_o$  and  $T_i$ , and left three free parameters  $f$ ,  $\kappa$  and  $\lambda$ , the free parameters at each site can be estimated by maximizing Nash-Sutcliffe model efficiency (NS).

**Table 1.** SLR and Tributary HSPF Contextual Information 2012

	<sup>1</sup> % Mine Water (min – max)	<sup>2</sup> % Groundwater (sample average)	<sup>3</sup> Transit Time (days; min – max)
SLR Skibo	N/A	100	0.3 – 12.3
SLR Forbes	1.0 – 40.3	89	5.2 – 40.0
SLR Mile 36	0.2 – 17.1	92	6.0 – 65.6
Whiteface R.	N/A	100	2.8 – 65.5
Cloquet R.	N/A	100	17.5 – 126.8
Floodwood R.	N/A	100	0.6 – 1.8
Swan R.	0.4 – 70.4	73	0.4 – 2.1
Partridge R.	1.4 – 56.5	81	7.5 – 51.4
Embarrass R.	3.2 – 40.5	83	14.7 – 95.2
West Two R.	6.6 – 100	54	1.8 – 87.3

<sup>1</sup> minimum occurs in the summer when dilution from background sources is high while maximum occurs in winter when background sources are low

<sup>2</sup> values represent the average percent groundwater on dates that samples were taken

<sup>3</sup> minimum transit times coincide with summer peak flows while maximum transit times occur during low flow and winter drought

## RIM Uncertainty Analysis

The difference between modeled and observed stream concentrations at individual sites was examined using NS:

$$NS = \left[ 1 - \frac{\sum_{t=1}^n (O_t - M_t)^2}{\sum_{t=1}^n (O_t - \bar{O})^2} \right] \quad (8)$$

where  $O_t$  is the observed concentration at time  $t$ ,  $M_t$  is the modeled concentration at time  $t$ , and  $\bar{O}$  is the average of the observed data throughout the comparison interval (Nash and

Sutcliffe, 1970). The index varies between negative infinity and one, where a NS equal to 1, 0 or negative values indicates, respectively, a perfect fit to the observed data, a fit equal to the observed mean, or a fit performing worse than the observed mean.

## Results

The relative distribution of source water was calculated at all ten sites revealing when and where different sources of water were dominant. Active groundwater was the overwhelmingly dominant source of water in the summer with intermittent rainfall events giving way to increasing proportions of surface runoff and interlayer flow for short intervals. Point source contributions increased in relative proportion during low flow conditions common in late summer, early fall and winter. Flow-weighted transit times were also calculated at all ten sites with the longest times occurring where large reservoirs exist somewhere in the tributary flow path (eg. Whiteface, Embarrass, West Two, Partridge and Cloquet Rivers) or where the SLR was receiving mixed contributions including those tributaries with large reservoirs (eg. SLR Mile 36).

Modeled porewater DOC, MeHg and THg concentrations for riparian soils decreased with depth indicated by positive  $f$  values at all sites. This type of soil profile is consistent with numerous observations in Swedish watersheds that reveal DOC, MeHg and THg porewater concentrations generally increasing toward the soil surface in riparian zones (Eklöf et al., 2015, Winterdahl et al., 2011, Seibert et al., 2009). However, the profile

for iron did not conform to the exponential shape and therefore  $c_o$  was allowed to vary as a free parameter at all sites when modeling dissolved iron. Dissolved iron concentrations in soils require reducing conditions to become elevated and so are not expected to be found in frequently unsaturated uppermost soil layers often in contact with atmospheric oxygen.

Graphical representations of the modeling results at each site can be found in Appendix 1. Observed DOC, MeHg and Fe peak stream concentrations occurred after a pronounced delay from peak spring flow conditions while THg peaks tended to coincide directly with peak flows regardless of season. After calibration of  $f$ ,  $\kappa$ , and  $\lambda$ , RIM was capable of predicting in-stream variations of DOC (NS = 0.06 to 0.78), MeHg (NS = 0.19 to 0.80), THg (NS = 0.35 to 0.86) and Fe (NS = 0.20 to 0.88) using streamflow as the main model driver and soil temperature as a time-varying parameter. Regression-based NS calculations were produced for DOC, THg and MeHg for seven of the ten modeled streams for comparison purposes (Table 2). Continuous flow records on a daily time step were not available for Floodwood, Embarrass or West Two Rivers, and as the most commonly used methods for regression-based load calculations rely on a continuous flow record to interpolate concentrations, NS values could not be calculated for those sites. Regression-based predictions calculated using the Army Corps of Engineers' FLUX32 software package offered an improvement compared to RIM for THg at SLR Skibo, Cloquet River and Swan River while RIM offered an improvement in all other cases (Table 2).

**Table 2.** Uncertainty analysis summary table. Those sites with an R contain large reservoirs. “FLUX” indicates reporting for regression-based results\* and NS values inside the black box may be compared directly. Superior NS values in the black box are underlined and in bold.

Site	MOD	NS <sub>RIM</sub>	NS <sub>FLUX</sub>
SLR Skibo	DOC	<b><u>0.73</u></b>	0.53
	MeHg	<b><u>0.80</u></b>	0.61
	THg	0.80	<b><u>0.87</u></b>
	Fe	<b><u>0.52</u></b>	
<sup>R</sup> SLR Forbes	DOC	<b><u>0.78</u></b>	0.61
	MeHg	<b><u>0.73</u></b>	0.31
	THg	<b><u>0.86</u></b>	0.67
	Fe	<b><u>0.88</u></b>	
<sup>R</sup> SLR Mile 36	DOC	<b><u>0.59</u></b>	0.42
	MeHg	<b><u>0.47</u></b>	0.01
	THg	<b><u>0.73</u></b>	0.53
	Fe	<b><u>0.60</u></b>	
<sup>R</sup> Whiteface	DOC	<b><u>0.41</u></b>	0.35
	MeHg	<b><u>0.35</u></b>	0.23
	THg	<b><u>0.72</u></b>	0.68
	Fe	<b><u>0.46</u></b>	
<sup>R</sup> Cloquet	DOC	<b><u>0.31</u></b>	0.11
	MeHg	<b><u>0.21</u></b>	0.13
	THg	0.47	<b><u>0.70</u></b>
	Fe	<b><u>0.38</u></b>	
Floodwood	DOC	<b><u>0.06</u></b>	
	MeHg	<b><u>0.24</u></b>	
	THg	<b><u>0.43</u></b>	
	Fe	<b><u>0.20</u></b>	
Swan	DOC	0.49	<b><u>0.52</u></b>
	MeHg	<b><u>0.19</u></b>	0.17
	THg	0.35	<b><u>0.70</u></b>
	Fe	<b><u>0.24</u></b>	
<sup>R</sup> Partridge	DOC	<b><u>0.52</u></b>	0.17
	MeHg	<b><u>0.72</u></b>	0.16
	THg	<b><u>0.66</u></b>	0.38
	Fe	<b><u>0.86</u></b>	
<sup>R</sup> Embarrass	DOC	<b><u>0.35</u></b>	
	MeHg	<b><u>0.67</u></b>	
	THg	<b><u>0.84</u></b>	
	Fe	<b><u>0.62</u></b>	
<sup>R</sup> West Two	DOC	<b><u>0.40</u></b>	
	MeHg	<b><u>0.57</u></b>	
	THg	<b><u>0.64</u></b>	
	Fe	<b><u>0.57</u></b>	

\*FLUX32 is Windows-based interactive software developed by Dave Soballe, U.S. Army Corps of Engineers (USACE), in conjunction with the Minnesota Pollution Control Agency. Using six calculation techniques, FLUX maps the flow/concentration relationship developed from the sample record onto the entire flow record to calculate total mass discharge and associated error statistics. In this study, concentrations were used and NS calculations were performed for comparison purposes. A full overview of FLUX32 methods can be found in the documentation that comes along with the software package (<https://www.pca.state.mn.us/wplmn/flux32>).

## Discussion

Concerns about MeHg levels throughout Minnesota create the need for a reliable and consistent means for predicting MeHg concentrations. Continuously monitoring MeHg concentration and loading at many sites throughout a watershed is cost- and labor-prohibitive. Thus, regulatory agencies often must rely on relatively few samples and use regression-based methods to characterize loading in a region. The reliability of such methods may be low, yet the consequences may be high in terms of economic cost for treatment or the potential to do environmental harm. Thus, the riparian zone modeling strategy, which links flow and chemistry together in glaciated boreal stream settings, provides opportunity for improvement in fitting chemistry to flow in the St. Louis River watershed, which is large and has relatively little data available for reactions taking place in the soils. With only data from streams (chemistry, flow and climate), RIM produces reliable predictions for at least a few important chemicals for many sites in the St. Louis River watershed. However, not all sites were found to be amenable to RIM and so it is important to consider where and what types of conditions contribute to either modeling success or added uncertainty.

First, it was found that RIM modeling results for the upper portions of the SLR main channel sites were among the best for the study. NS values for all chemicals ranged from 0.73 to 0.88 at both SLR Skibo and SLR Forbes, excluding only iron at SLR Skibo, which had NS value of 0.52. The model for SLR Mile 36 had considerably lower predictive power for all four chemicals owing likely to increasing size of its drainage area, the

influence of increased residence times and extensive mixing of waters derived from different settings (mines, reservoirs, streams). Whiteface and Cloquet Rivers have very similar hydrologic conditions and landscape composition and resulted in similar modeling results with lower predictive power likely due to longer transit times and reservoir influences. Due to the size of these tributaries and the presence of reservoirs along the flow path, the time between averaged recharge and sampling is longer in these watersheds and so the opportunity for in-stream modifications to chemistry is larger. RIM modeling had difficulty predicting chemistry for these sites, but still had predictive power equal to or, in most cases, greater than the simple regression models. Modeling of Floodwood River was complicated by a significant number of data gaps. Flow measurements were missing for four of the fifteen samples creating serious issues for chemistry predictions. Swan River, which very similar in most other ways, did not have those flow data gaps and the model predicted chemistry considerably better. The contrast between these two similar sites highlighted the importance of data continuity when using RIM. Partridge, Embarrass and West Two Rivers had NS values for all chemicals ranging from 0.35 to 0.86 with DOC models performing the worst owing likely to very strong mine influences and/or long flow paths with ample opportunity for degradation (Table 1). An inherent difficulty of this modeling approach is the level of trust that must be placed in HSPF's ability to calculate stream composition. An interesting follow-up to the current study could involve the comparison of RIM modeling using a further calibrated version of HSPF, with the assumption that its ability to make stream composition calculations had improved with additional data, with the current RIM modeling results.

Models for smaller drainage areas with lower transit times performed better than those with large drainage areas and lengthy transit times. Lower transit times indicate that the site is controlled more heavily by local groundwater inputs under more uniform conditions while longer transit times indicate possibly an important influence of surface exposure and chemical transformation in the water column. HSPF was used to characterize storage time, but in-stream and lake reactions were not explicitly modeled in this study. Specific ultraviolet absorbance (SUVA), which was measured in 2012 and 2013, provides a possible means for capturing water column processes. Ultraviolet absorption at 254 nanometers ( $UV_{254}$ ) corrected for dissolved iron content was used to determine SUVA which is the  $UV_{254}$  absorbance divided by DOC concentration (Burns et al., 2013, Berndt et al., 2014). SUVA calculated in this way represents the aromaticity of the DOC and serves as a proxy for DOC age in the water column. In general, higher SUVA values tend to coincide with gentler slopes and greater riparian influence while lower SUVA values indicate a greater influence of open water with biotic (microbial cycling) and/or abiotic (photodegradation) transformation due to prolonged surface exposure of DOC (Burns et al., 2013). SUVA also serves as an indication of DOC source and so careful interpretation is needed.

Comparing SUVA to HSPF transit times does help identify some possible trends occurring throughout the watershed. The general seasonal tendencies of DOC aromaticity (SUVA) as it enters the stream could be observed at the confluences at sites with very low transit times (SLR Skibo, Floodwood River and Swan River). Early in the season, when microbial activity was likely to be just ramping up and old porewater was being mobilized,

lower SUVA values were observed. SUVA then peaked in mid-summer when microbial activity is usually high, producing fresh, aromatic DOC, and groundwater flow paths were likely accessing less altered DOC in shallower zones. As flows again begin to decline, water from more reduced zones were likely flushed into the river bringing more heavily altered DOC. Where transit times were long due to stream length and the presence of reservoir storage along the flowpath, SUVA values tended to vary much less than areas where stream flushing was occurring more regularly. This tended to dampen the seasonal variation of SUVA and create a steadier, less variable SUVA trend throughout the season.

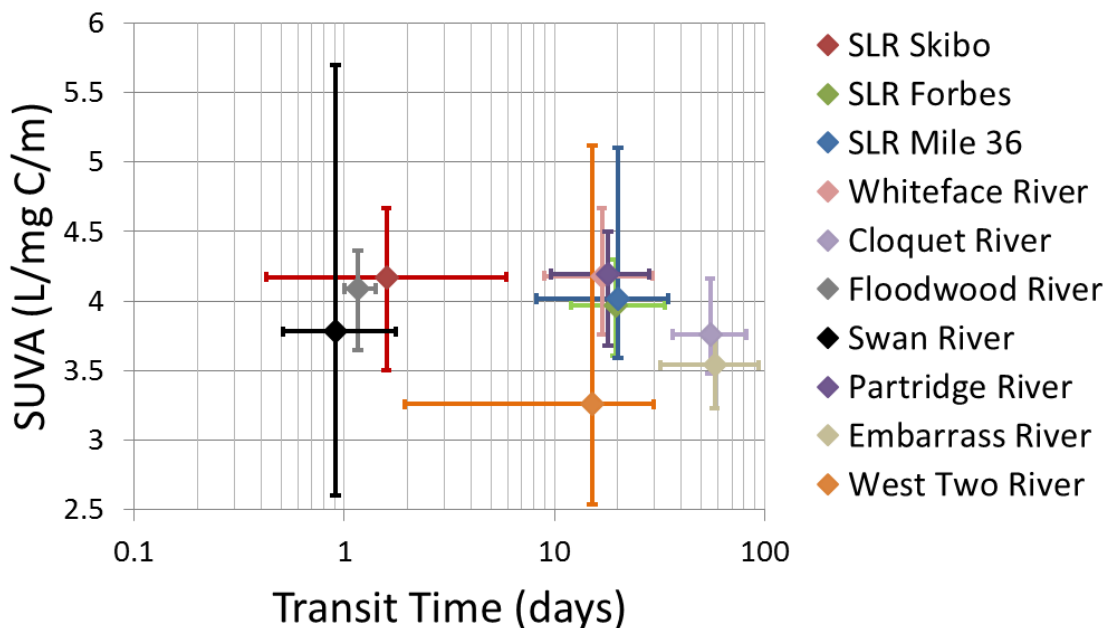


**Figure 5.** Specific Ultraviolet Absorbance vs. HSPF calculated flow-weighted transit times. Vertical bars represent the range of observed SUVA values at each site while horizontal bars similarly represent the range of transit times calculated on sampling days.

Knowing SUVA values at the confluences alone does not provide enough information to interpret the level to which waters have transformed along their flow path. However,

SUVA values at the confluences combined with SUVA information from headwaters and knowledge of transit times may provide a means for developing degradation coefficients that could be implemented in HSPF. Such a formulation may allow for the characterization of upstream inputs more thoroughly and improve future RIM calculations in streams with long transit times.

This model was developed and is used here in a relatively flat, glaciated landscape, and the simplified principles may not hold true in landscapes with significantly higher relief and increasing proportions of surface runoff. Surface runoff was ignored in this study in order to focus on riparian groundwater influences. The oxidizing conditions associated with direct surface runoff would not be expected to produce high MeHg waters and likely have a minimal effect on MeHg loading to the river. The relative contribution of surface runoff can be conceptualized by plotting HSPF tracer concentrations alongside active groundwater and interlayer flow through time (Figure 3). While the relative distribution does show significant surface inputs immediately following precipitation events, their presence in the river is short-lived and does not coincide with peak MeHg concentrations.

Long term climate change may have an effect on soil and runoff characteristics for different land types and which could call for more thorough treatments of the surface runoff component. While temperature was included here as a dynamic model parameter, soil wetness, vegetation type and cover, and variability of microbial activity associated with soil wetness and vegetation change could also potentially be used as dynamic variables in future iterations.

The RIM strategy was in most cases an improvement compared to regression-based modeling techniques (Table 2). Daily loading rates could be calculated similarly to regression methods with RIM results by extending the flow record for the entire season and using parameter values calculated using the sample record to interpolate stream chemistry. In that way the two methods perform very similarly differing only in RIM's more physically based methods. More chemical and flow data would certainly help to further constrain the model parameters and allow the RIM strategy to be carried out for a calibrated watershed using only relatively inexpensive flow measurements. This would provide a consistent means for predicting mercury contamination in fish using RIM to predict mercury loads and empirical bioaccumulation factors to calculate fish concentrations. In this study, RIM models were not developed for tributaries that lacked stream chemistry and flow since to do so would require considerable assumptions and result in great uncertainties. The parameters used for these specific tributaries and SLR sites (Appendix 2) vary widely and so more work is needed to extrapolate the fitted parameters elsewhere with confidence.

An important objective of the present study was to relate chemistry to flow using the least number of fit parameters possible. To do this, the equations being used to provide the chemistry fit to changing conditions must at least approximate the actual processes that occur in the system. Simple linear regression curves work well for the mixing of two end member solutions, but in this system, where DOC, THg, MeHg, and Fe concentrations respond rapidly to changing flow patterns and in temperature dependent fashion, greater

sophistication is required. It is important to note that regression-based and RIM methods are not the only attempts at modeling MeHg in the SLR. On the other end of the spectrum, an explicit, physically-based model has been developed for this watershed. Specifically, the watershed model WARMF was used to model everything from landscape and soil reactive transport to in-stream reaction and bioaccumulation in the SLR (RTI, 2013). This WARMF modeling attempt was frustrated by a lack of needed data, including transport and source terms that specifically relate flow to MeHg chemistry.

HSPF and RIM appear to be ideally matched to combine simplicity and complexity into one modeling strategy. Both models assume that the majority of precipitation that falls on the watershed is transported through shallow groundwater systems and assume that recharge occurs through the riparian zones. HSPF provides a means to superimpose immense data sets representing climatic conditions onto a large, diverse landscape to predict flow, and RIM provides a simple mechanism to convert that flow into stream chemistry. Together, and with measurement of relatively few samples, the tools can be combined to provide improved approximation of loading of important chemicals. The improved fits obtained here for the RIM model using measured flow data and the HSPF characterizations show that combining the techniques has great promise in northern Minnesota and elsewhere.

## Conclusions

RIM modeling techniques provide a means to assess how chemistry in riparian zone porewater is influencing stream chemistry. Chemical profiles in the riparian zone were modeled using observed streamflow and stream chemistry as the main constraints. Stream chemistries could then be represented as simple functions of flow using a relatively few number of parameters to characterize the individual tributaries and main river sites. This study also provided a more robust strategy for modeling constituent loads compared to a simple empirical regression model that did not incorporate soil temperature as a dynamic variable. Sites with lower flow-weighted transit times and less impact from lakes had better performing RIM models while those with data gaps and lakes that tie up water for long periods of time during the wet season tend to perform worse. While the landscape in this study is in general large and heterogeneous with a complex combination of varying hillslopes, wetlands, lakes and mining influences, RIM in combination with HSPF nevertheless provided feasible explanations for variation in stream chemistry without examining those components individually.

Recognition and use of RIM would ideally allow catchment modeling to capture natural and anthropogenic influences that may be blurring our understanding of natural processes. This study also shows the utility of using the Riparian Flow-Concentration Integration Modeling method in other important landscapes throughout North America and bring to light the importance of the riparian zone and its basic influence on relationships between climate, hydrology, biology and geology for predicting stream chemistry. At the

watershed scale, this simple method offers a means to step back from ever-increasingly complex watershed scale simulations while still emphasizing the few basic governing processes.

## References

- Atkeson, T., Axelrod, D., Pollman, C. and Keeler, G. (2003) *Integrating Atmospheric Mercury Deposition and Aquatic Cycling in the Florida Everglades: An approach for conducting a Total Maximum Daily Load analysis for an atmospherically derived pollutant*, Florida Department of Environmental Protection.
- Bailey, L., Johnson, N., Mitchell, C., Engstrom, D., Berndt, M. and Coleman-Wasik, J. (2014a) *Geochemical factors influencing methylmercury production and partitioning in sulfate-impacted lake sediments*, Minnesota Department of Natural Resources.
- Bailey, L., Johnson, N., Mitchell, C., Engstrom, D., Coleman-Wasik, J., Kelly, M. and Berndt, M. (2014b) *Seasonal and spatial variations in methylmercury in the water column of sulfate impacted lakes*, Minnesota Department of Natural Resources.
- Benoit, J. M. (1999) 'Sulfide controls on mercury speciation and bioavailability to methylating bacteria in sediment pore waters', *Environmental Science and Technology*, 33(6), pp. 951-957.
- Berndt, M. and Bavin, T. (2009) *Sulfate and Mercury Chemistry of the St. Louis River in Northeastern Minnesota*, Minnesota Department of Natural Resources; Minerals Coordinating Committee.
- Berndt, M. and Bavin, T. (2011) *Sulfate and Mercury Cycling in Five Wetlands and a Lake Receiving Sulfate from Taconite Mines in Northeastern Minnesota*, Minnesota Department of Natural Resources.
- Berndt, M., Jeremiason, J. and Von Korff, B. (2014) *Hydrologic and Geochemical Controls on St. Louis River Chemistry with Implications for Regulating Sulfate to Control Methylmercury Concentrations*, Minnesota Department of Natural Resources; Environmental Natural Resources Trust Fund.
- Berndt, M. E. and Bavin, T. K. (2012) 'Methylmercury and dissolved organic carbon relationships in a wetland-rich watershed impacted by elevated sulfate from mining', *Environmental Pollution*, 161, pp. 321.

- Berndt, M. E., Rutelonis, W. and Regan, C. P. (2016) 'A comparison of results from a hydrologic transport model ( HSPF) with distributions of sulfate and mercury in a mine- impacted watershed in northeastern Minnesota', *Journal of Environmental Management*, 181, pp. 74-79.
- Bicknell, B. R., Imhoff, J. C., Kittle Jr., J. L., Jobes, T. H. and Donigian Jr., A. S. (2005) *Hydrological Simulation Program - Fortran User's Manual: Version 12.2*, United States Environmental Protection Agency and United States Geological Survey: Aqua Terra Consultants.
- Bishop, K., Seibert, J., Köhler, S. and Laudon, H. (2004) 'Resolving the Double Paradox of rapidly mobilized old water with highly variable responses in runoff chemistry', *Hydrological Processes*, 18(1), pp. 185-189.
- Bradley, P. M., Journey, C. A., Lowery, M. A., Brigham, M. E., Burns, D. A., Button, D. T., Chapelle, F. H., Lutz, M. A., Marvin-Dipasquale, M. C. and Riva-Murray, K. (2012) 'Shallow groundwater mercury supply in a Coastal Plain stream', *Environmental science & technology*, 46(14), pp. 7503.
- Burns, D., Aiken, G., Bradley, P., Journey, C. and Schelker, J. (2013) 'Specific ultra- violet absorbance as an indicator of mercury sources in an Adirondack River basin', *Biogeochemistry*, 113(1), pp. 451-466.
- Coleman Wasik, J. K., Mitchell, C. P. J., Engstrom, D. R., Swain, E. B., Monson, B. A., Balogh, S. J., Jeremiason, J. D., Branfireun, B. A., Eggert, S. L., Kolka, R. K. and Almendinger, J. E. (2012) 'Methylmercury declines in a boreal peatland when experimental sulfate deposition decreases', *Environmental science & technology*, 46(12), pp. 6663.
- Compeau, G. C. and Bartha, R. (1985) 'Sulfate- Reducing Bacteria: Principal Methylators of Mercury in Anoxic Estuarine Sediment', *Applied and Environmental Microbiology*, 50(2), pp. 498.
- Eklöf, K., Kraus, A., Futter, M., Schelker, J., Meili, M., Boyer, E. W. and Bishop, K. (2015) 'Parsimonious Model for Simulating Total Mercury and Methylmercury in Boreal Streams Based on Riparian Flow Paths and Seasonality', *Environ. Sci. Technol.*, pp. 150625085250006.

- Engstrom, D. R. (2007) 'Fish Respond When the Mercury Rises', *Proceedings of the National Academy of Sciences of the United States of America*, 104(42), pp. 16394-16395.
- Engstrom, D. R. and Swain, E. B. (1997) 'Recent declines in atmospheric mercury deposition in the Upper Midwest', *Environmental Science & Technology*, 31(4), pp. 960.
- Gilmour, C. C., Henry, E. A. and Mitchell, R. (1992) 'Sulfate stimulation of mercury methylation in freshwater sediments', *Environ. Sci. Technol.*, 26(11), pp. 2281-2287.
- Jeremiason, J., Reiser, T., Weitz, R., Berndt, M. and Aiken, G. (2016) 'Aeshnid dragonfly larvae as bioindicators of methylmercury contamination in aquatic systems impacted by elevated sulfate loading', *Ecotoxicology*, 25(3), pp. 456-468.
- Jeremiason, J., Walker, M., Voigt, B. and Aiken, G. (2014b) *Binding of MeHg to Dissolved Organic Matter*, Minnesota Department of Natural Resources.
- Jeremiason, J. D., Engstrom, D. R., Swain, E. B., Nater, E. A., Johnson, B. M., Almendinger, J. E., Monson, B. A. and Kolka, R. K. (2006) 'Sulfate addition increases methylmercury production in an experimental wetland', *Environmental science & technology*, 40(12), pp. 3800.
- Jeremiason, J. D., Portner, J. C., Aiken, G. R., Hiranaka, A. J., Dvorak, M. T., Tran, K. T. and Latch, D. E. (2015) 'Photoreduction of Hg( ii ) and photodemethylation of methylmercury: the key role of thiol sites on dissolved organic matter', *Journal of Environmental Monitoring*, 17(11), pp. 1892-1903.
- Johnson, N. W., Mitchell, C. P. J., Engstrom, D. R., Bailey, L. T., Coleman Wasik, J. K. and Berndt, M. E. (2016) 'Methylmercury production in a chronically sulfate-impacted sub- boreal wetland', *Journal of Environmental Monitoring*, 18(6), pp. 725-734.
- Ledesma, J. L. J., Futter, M. N., Laudon, H., Evans, C. D. and Köhler, S. J. (2016) 'Boreal forest riparian zones regulate stream sulfate and dissolved organic carbon', *Science of the Total Environment*, 560-561, pp. 110-122.
- Mason, R. P., Abbott, M. L., Bodaly, R. A., Bullock, O. R., Driscoll, C. T., Evers, D., Lindberg, S. E., Murray, M. and Swain, E. B. (2005) 'Monitoring the response to

- changing mercury deposition', *Environmental science & technology*, 39(1), pp. 14A.
- Meili, M., Bishop, K., Bringmark, L., Johansson, K., Munthe, J., Sverdrup, H. and de Vries, W. (2003) 'Critical levels of atmospheric pollution: criteria and concepts for operational modelling of mercury in forest and lake ecosystems', *Science of the Total Environment*, 304(1), pp. 83-106.
- MPCA (2007) *Minnesota Statewide Mercury Total Maximum Daily Load*, Minnesota Pollution Control Agency.
- Munthe, J., Branfireun, B. A., Driscoll, C. T., Gilmour, C. C., Horvat, M., Lucotte, M. and Malm, O. (2007) 'Recovery of Mercury- Contaminated Fisheries', *Ambio*, 36(1), pp. 33-44.
- Nash, J. E. and Sutcliffe, J. V. (1970) 'River flow forecasting through conceptual models part I — A discussion of principles', *Journal of Hydrology*, 10(3), pp. 282-290.
- Paola, C. (2011) 'Environmental dynamics: Simplicity versus complexity', *Nature*, 469(7328), pp. 38.
- Parks, J. M., Johs, A., Podar, M., Bridou, R., Hurt, J. R. A., Smith, S. D., Tomanicek, S. J., Qian, Y., Brown, S. D., Brandt, C. C., Palumbo, A. V., Smith, J. C., Wall, J. D., Elias, D. A. and Liang, L. (2013) 'The Genetic and Enzymatic Basis of Bacterial Mercury Methylation', *Science*, 339(6125).
- Poulain, A. J. and Barkay, T. (2013) 'Environmental science. Cracking the mercury methylation code', *Science (New York, N.Y.)*, 339(6125), pp. 1280.
- Rolfhus, K., Hall, B., Monson, B., Paterson, M. and Jeremiason, J. (2011) 'Assessment of mercury bioaccumulation within the pelagic food web of lakes in the western Great Lakes region', *Ecotoxicology*, 20(7), pp. 1520-1529.
- RTI (2013) *St. Louis River Estuary TMDL Project, Preliminary WARMF Modeling Report*, United States Environmental Protection Agency.
- Schroeder, W. H., Anlauf, K. G., Barrie, L. A., Lu, J. Y., Steffen, A., Schneeberger, D. R. and Berg, T. (1998) 'Arctic springtime depletion of mercury', *Nature*, 394(6691), pp. 331.

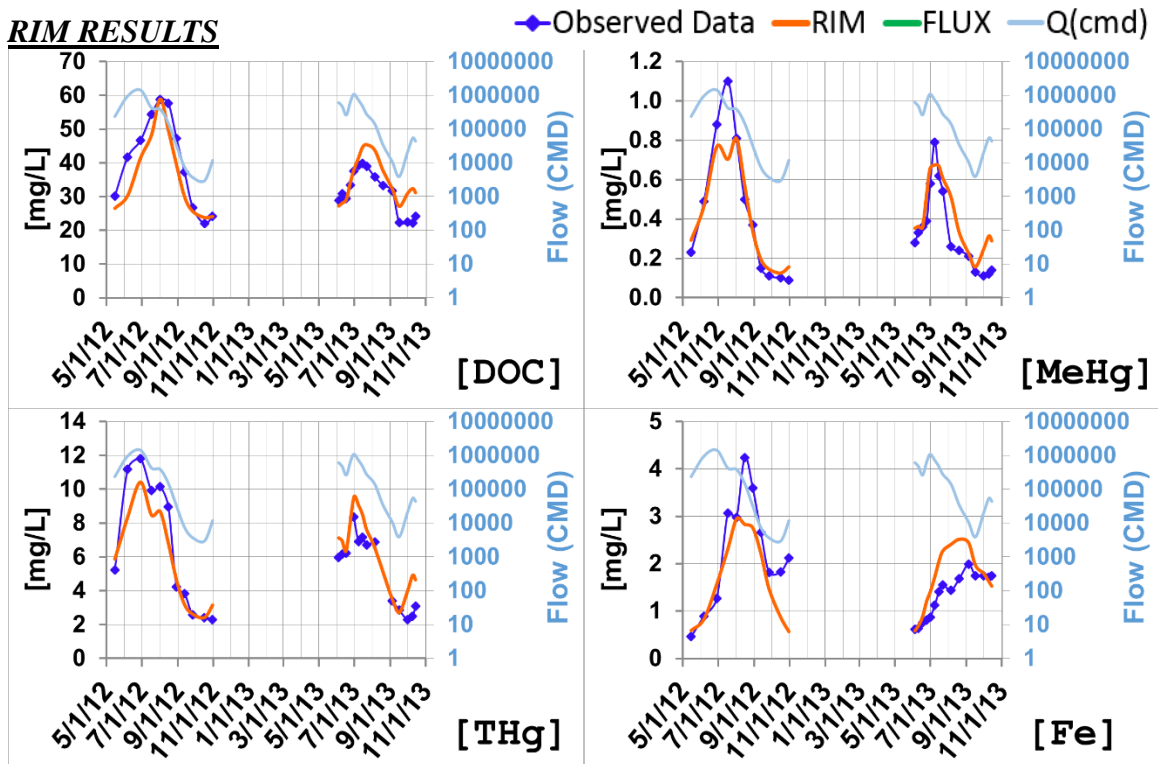
- Seibert, J., Grabs, T., Kohler, S., Laudon, H., Winterdahl, M. and Bishop, K. (2009) 'Linking soil- and stream-water chemistry based on a Riparian Flow-Concentration Integration Model', *Hydrology And Earth System Sciences*, 13(12), pp. 2287-2297.
- Skyllberg, U. (2008) 'Competition among thiols and inorganic sulfides and polysulfides for Hg and MeHg in wetland soils and sediments under suboxic conditions: Illumination of controversies and implications for MeHg net production', *Journal of Geophysical Research: Biogeosciences*, 113(G2), pp. n/a-n/a.
- Skyllberg, U. and Drott, A. (2010) 'Competition between Disordered Iron Sulfide and Natural Organic Matter Associated Thiols for Mercury( II)-An EXAFS Study', *Environmental Science & Technology*, 44(4), pp. 1254-1259.
- Swain, E. B. (1992) 'Increasing rates of atmospheric mercury deposition in midcontinental North America', *Science*, 257(5071).
- TetraTech (2013) *St. Louis, Cloquet, and Nemadji River Basins - Hydrologic Model Calibration*, Minnesota Pollution Control Agency.
- Watras, C. J., Back, R. C., Halvorsen, S., Hudson, R. J. M., Morrison, K. A. and Wente, S. P. (1998) 'Bioaccumulation of mercury in pelagic freshwater food webs', *Science of the Total Environment*, 219(2), pp. 183-208.
- Winterdahl, M., Erlandsson, M., Futter, M. N., Weyhenmeyer, G. A. and Bishop, K. (2014) 'Intra- annual variability of organic carbon concentrations in running waters: Drivers along a climatic gradient', *Global Biogeochemical Cycles*, 28(4), pp. 451-464.
- Winterdahl, M., Futter, M., Köhler, S., Laudon, H., Seibert, J. and Bishop, K. (2011) 'Riparian soil temperature modification of the relationship between flow and dissolved organic carbon concentration in a boreal stream', *Water Resources Research*, 47(8), pp. n/a-n/a.

## **Appendix 1**

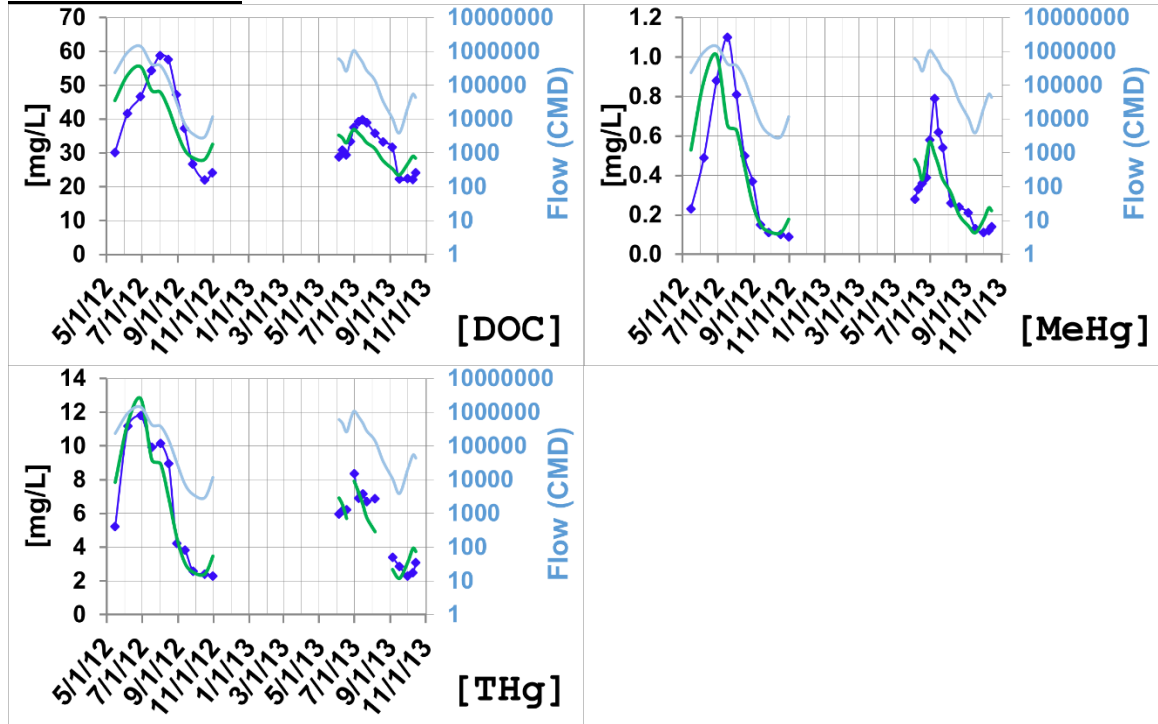
### RIM and FLUX Modeling Results

*St. Louis River – Mile 179 (Skibo)*

**RIM RESULTS**

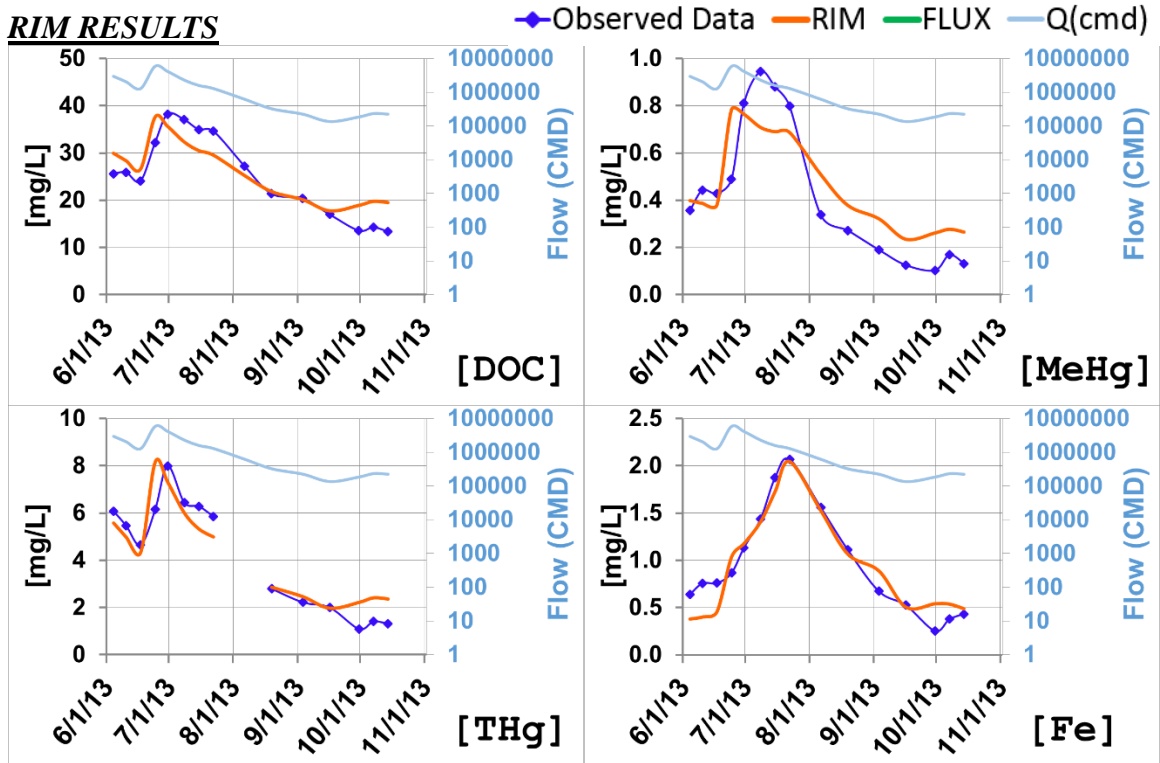


**FLUX RESULTS**

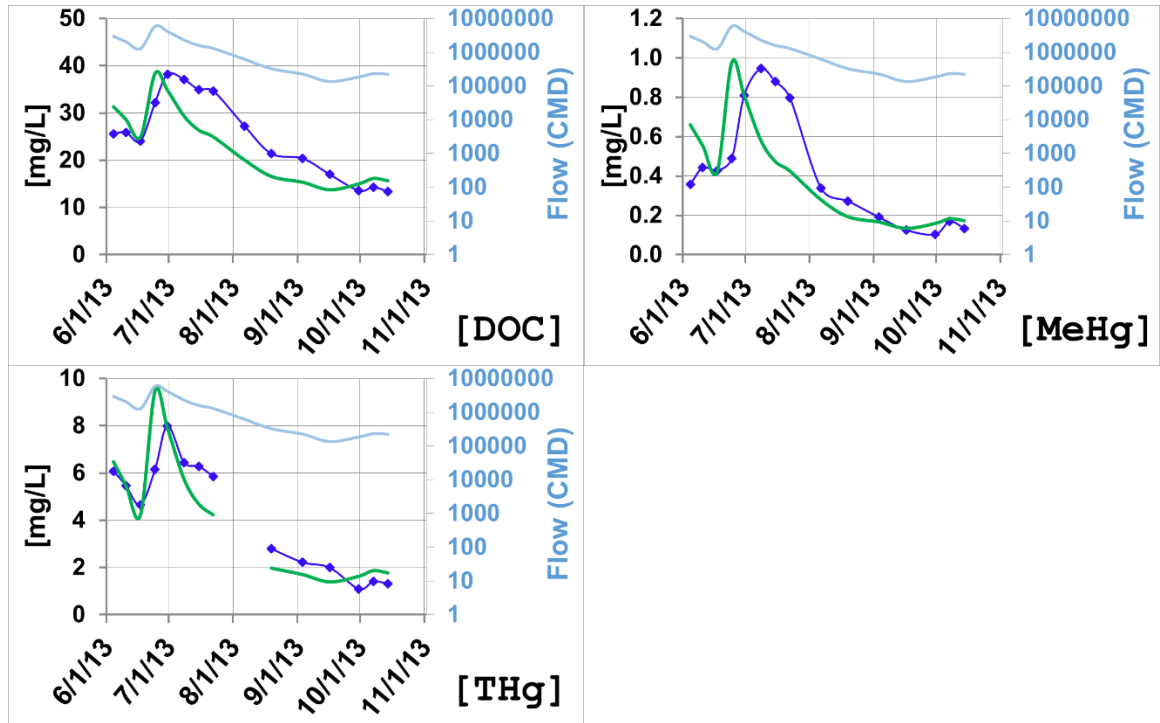


*St. Louis River – Mile 94 (Forbes)*

**RIM RESULTS**



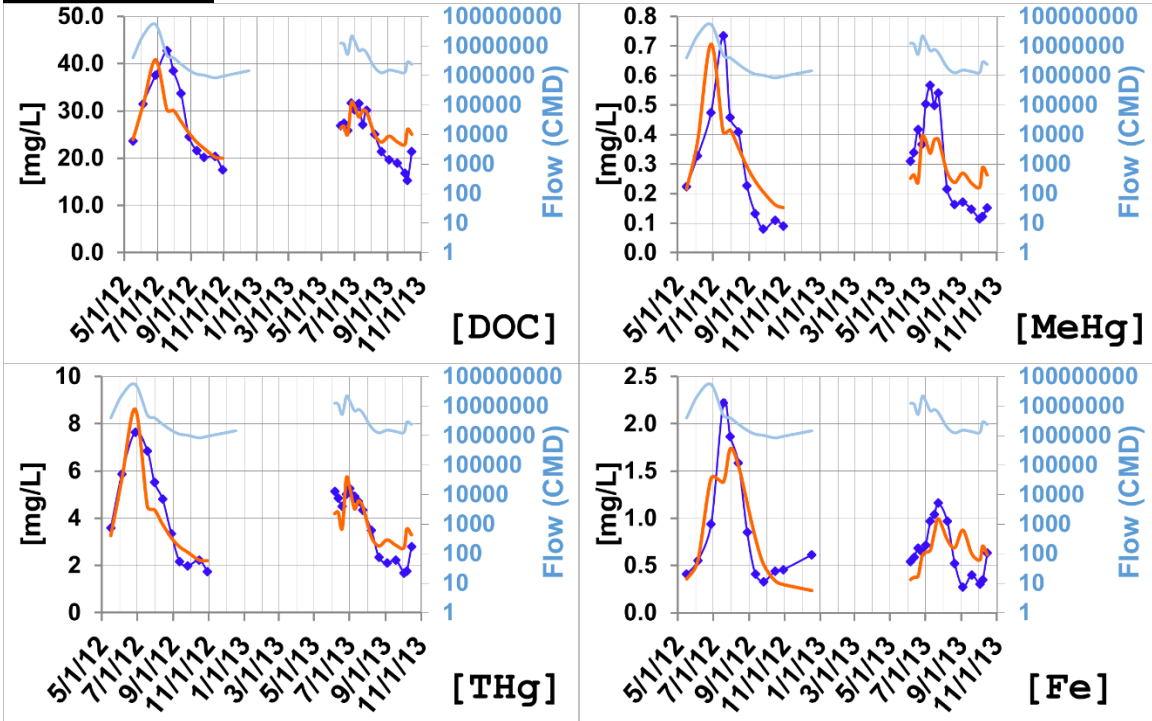
**FLUX RESULTS**



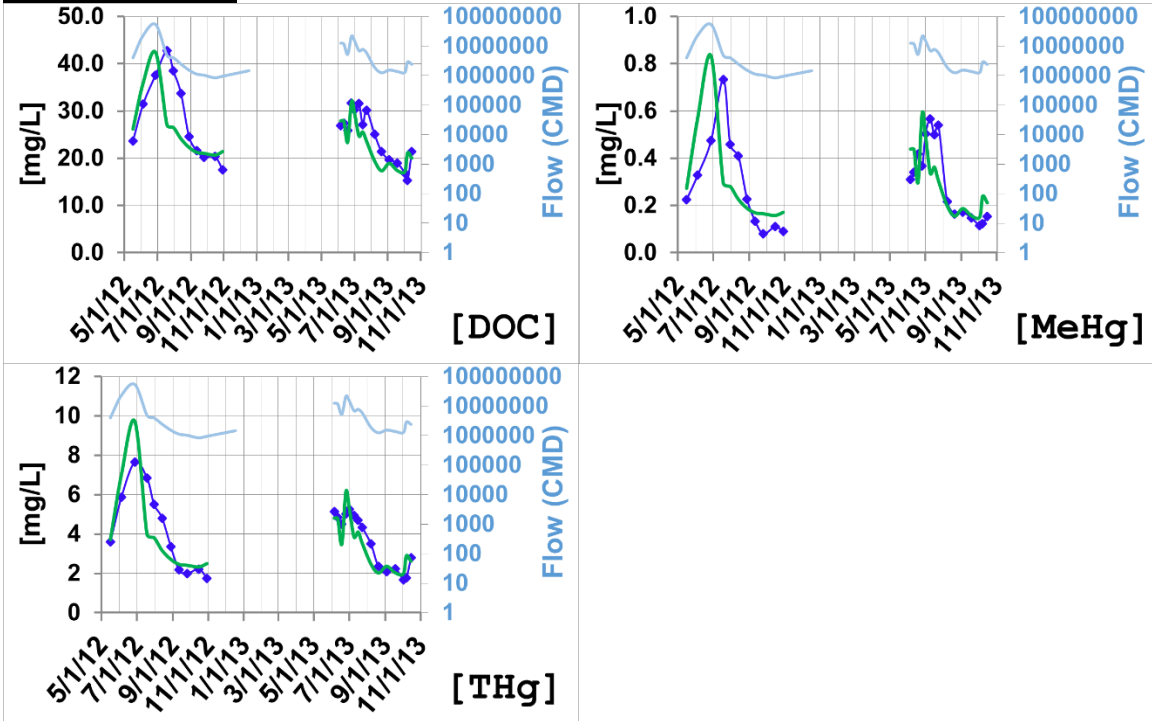
St. Louis River – Mile 36

**RIM RESULTS**

◆ Observed Data    — RIM    — FLUX    — Q(cmd)



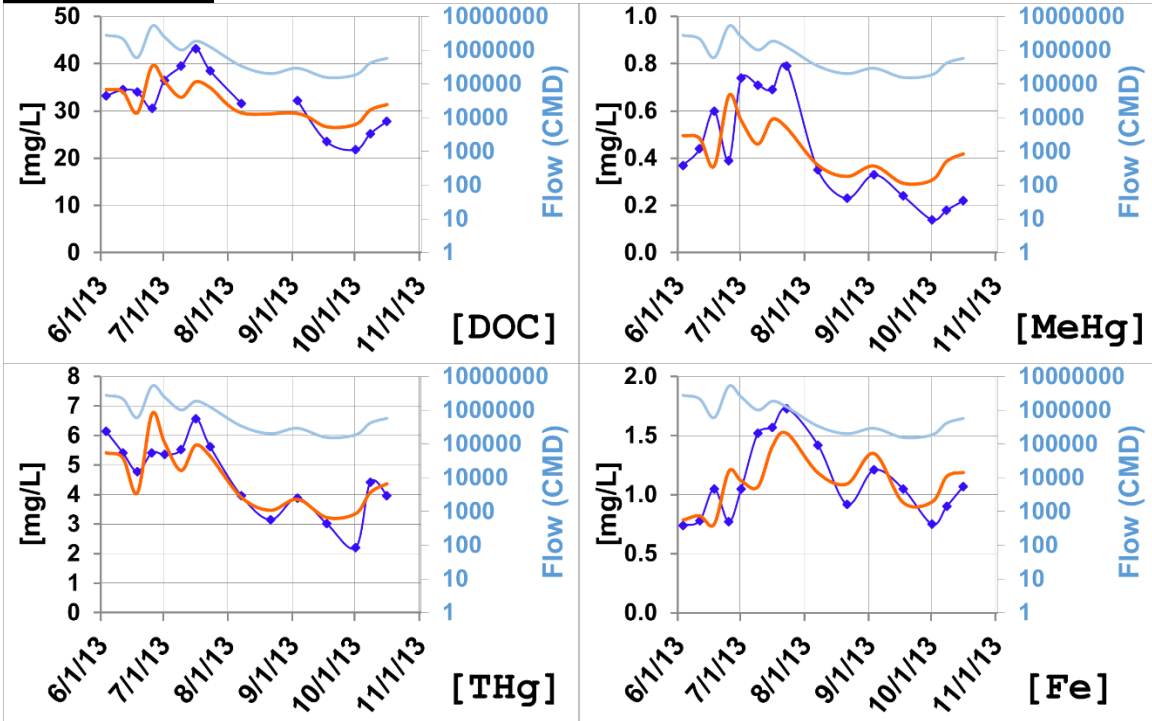
**FLUX RESULTS**



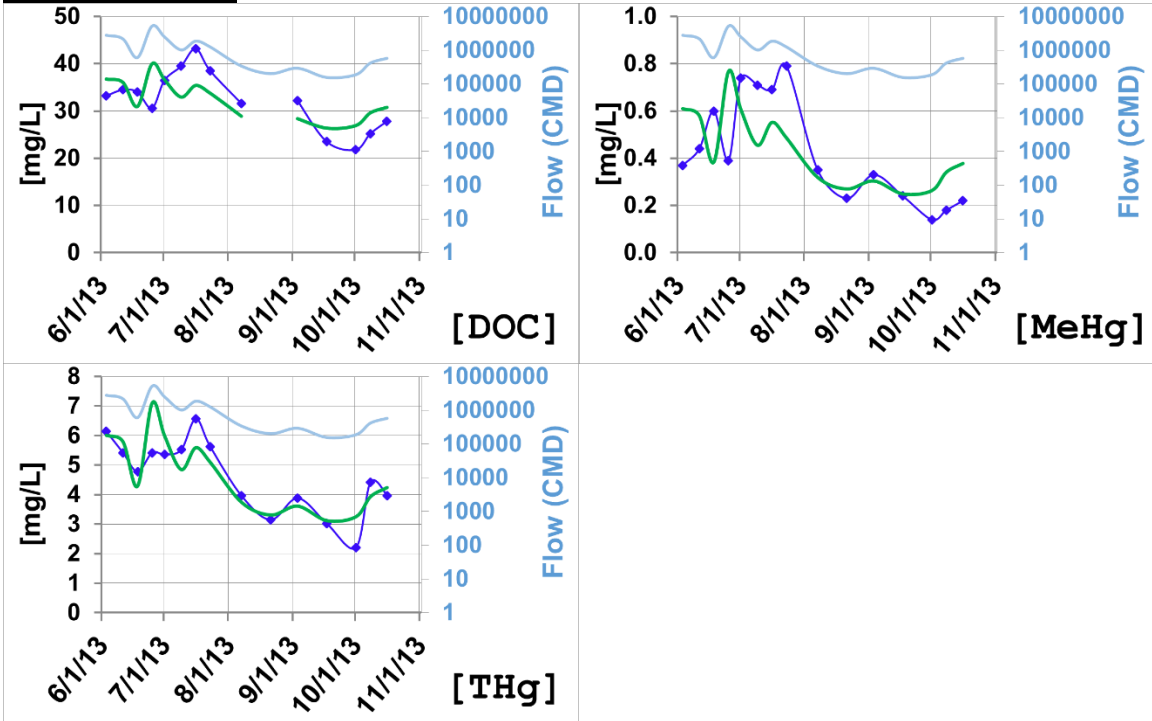
## Whiteface River

### RIM RESULTS

◆ Observed Data    — RIM    — FLUX    — Q(cmd)

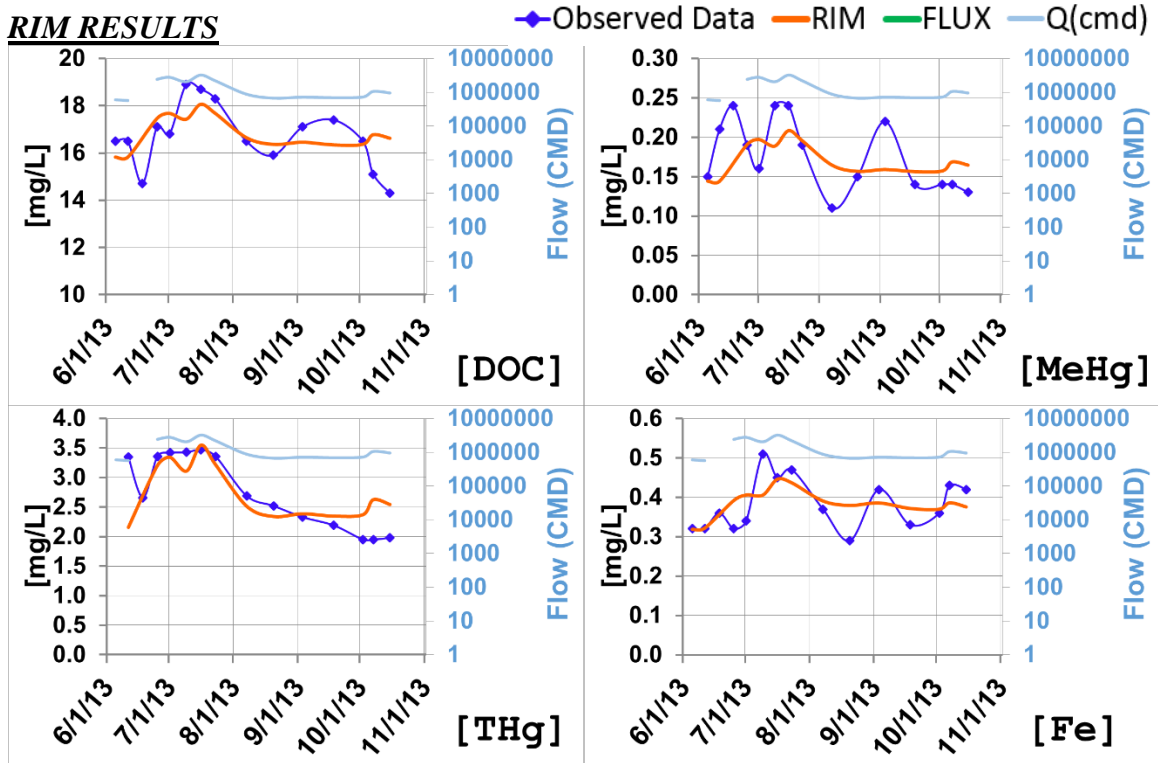


### FLUX RESULTS

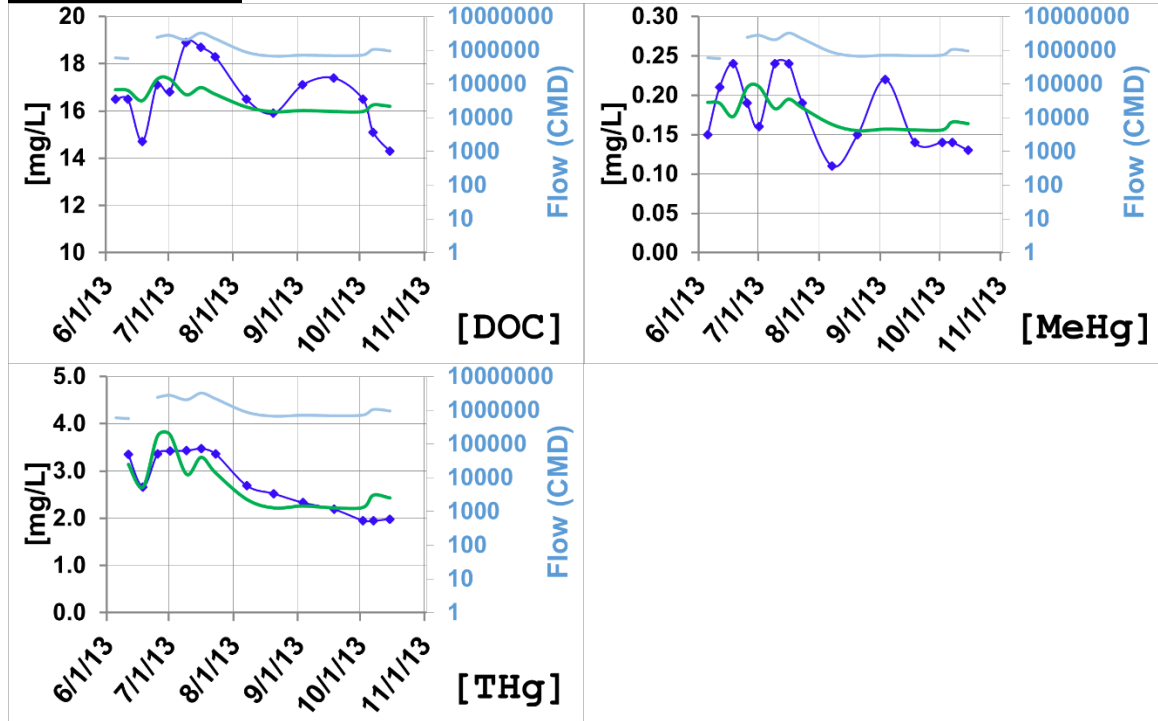


## Cloquet River

### RIM RESULTS



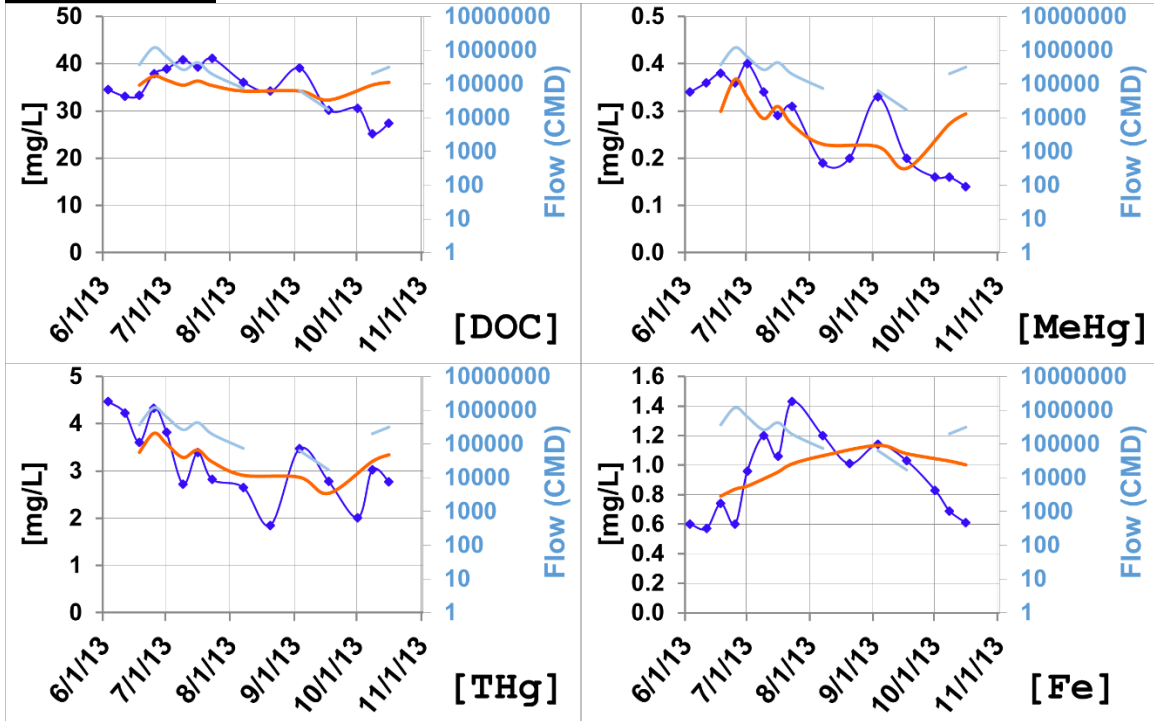
### FLUX RESULTS



## Floodwood River

### RIM RESULTS

◆ Observed Data    — RIM    — FLUX    — Q(cmd)

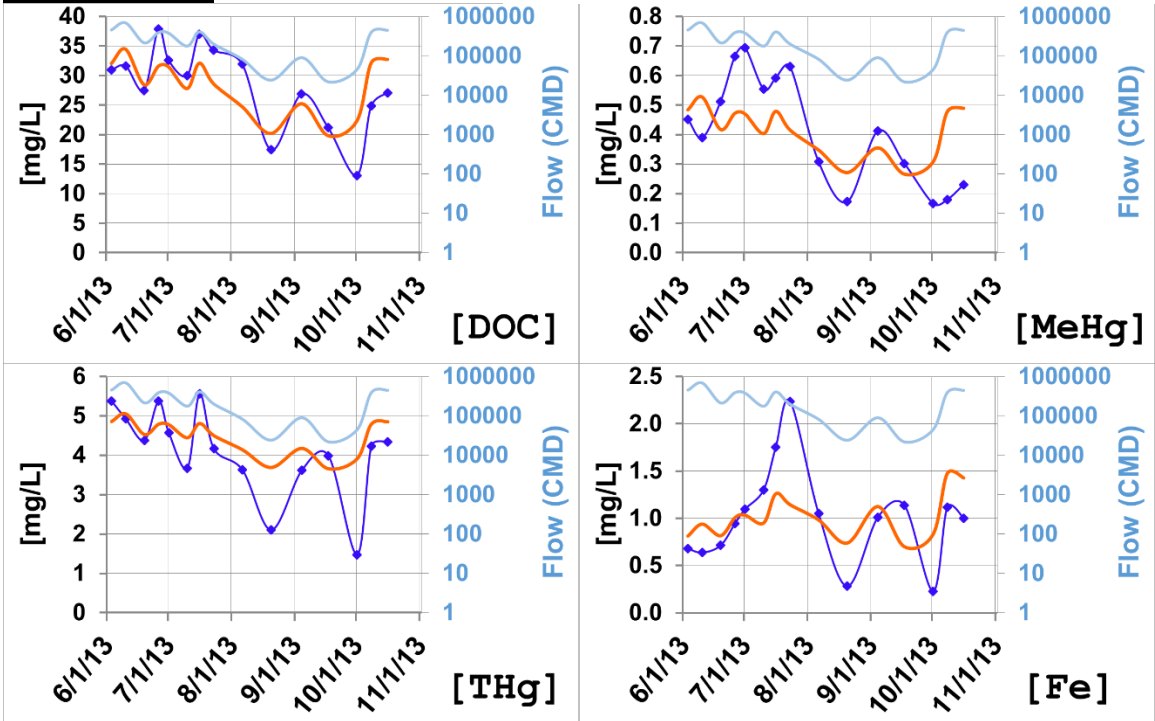


NO FLUX RESULTS AVAILABLE

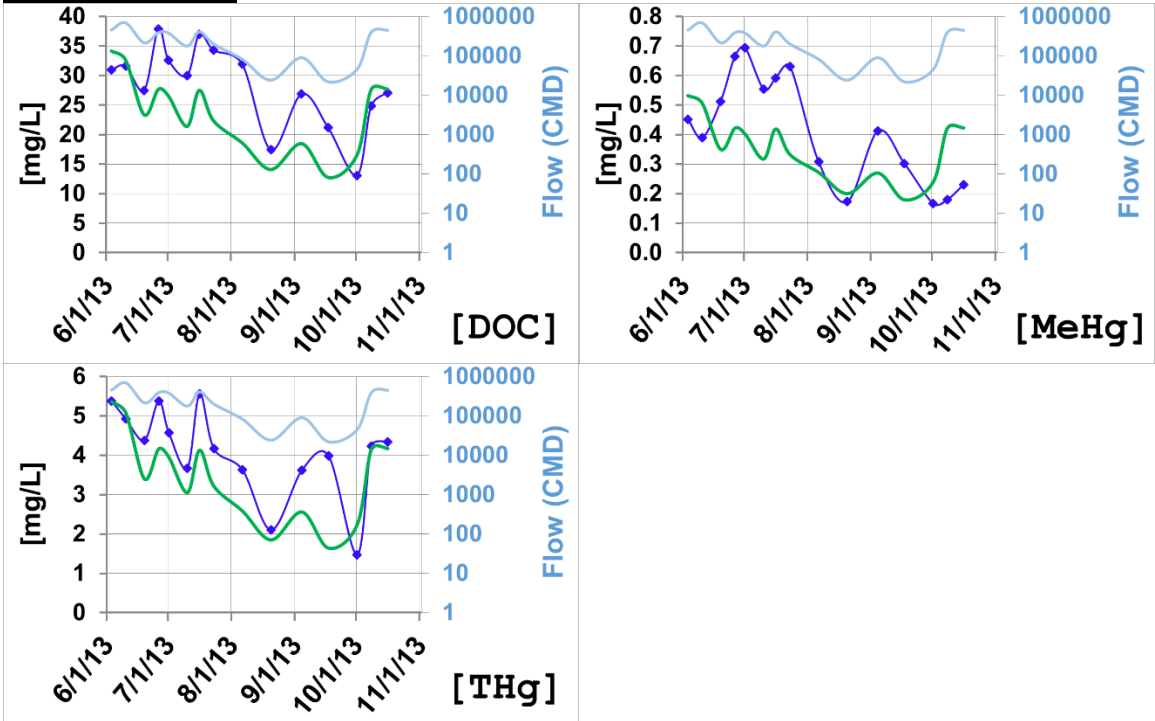
## Swan River

### RIM RESULTS

◆ Observed Data    — RIM    — FLUX    — Q(cmd)

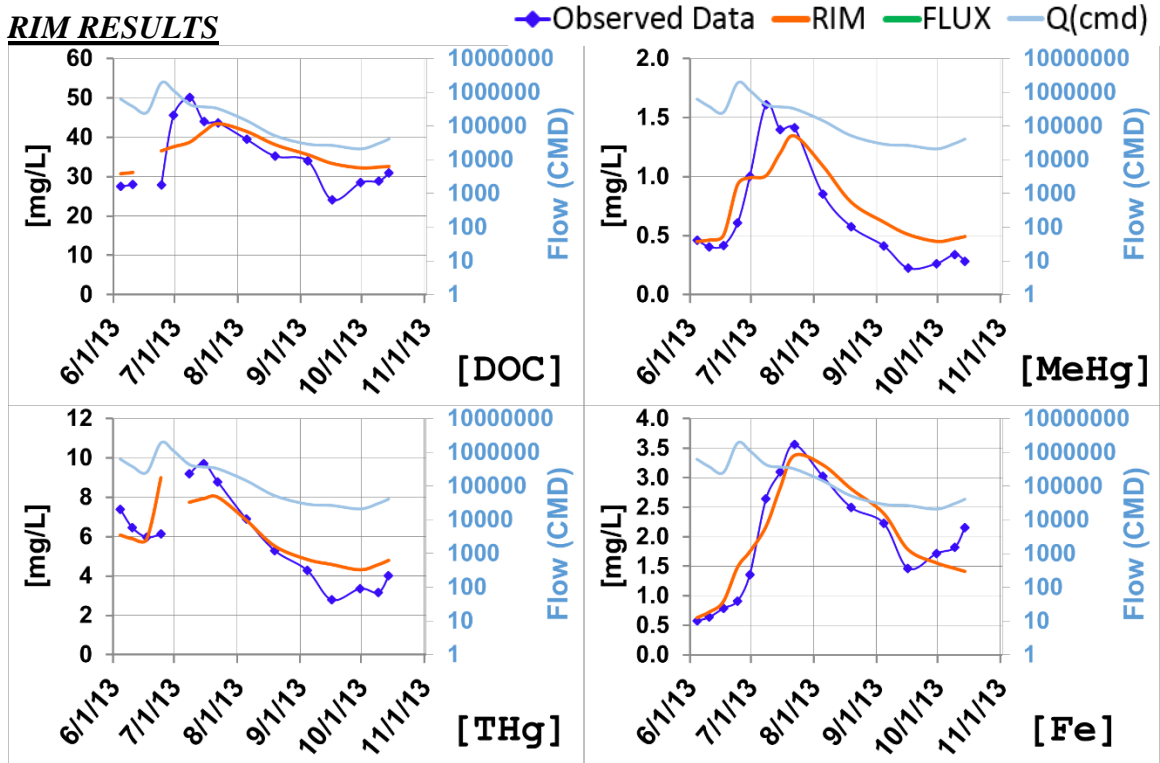


### FLUX RESULTS

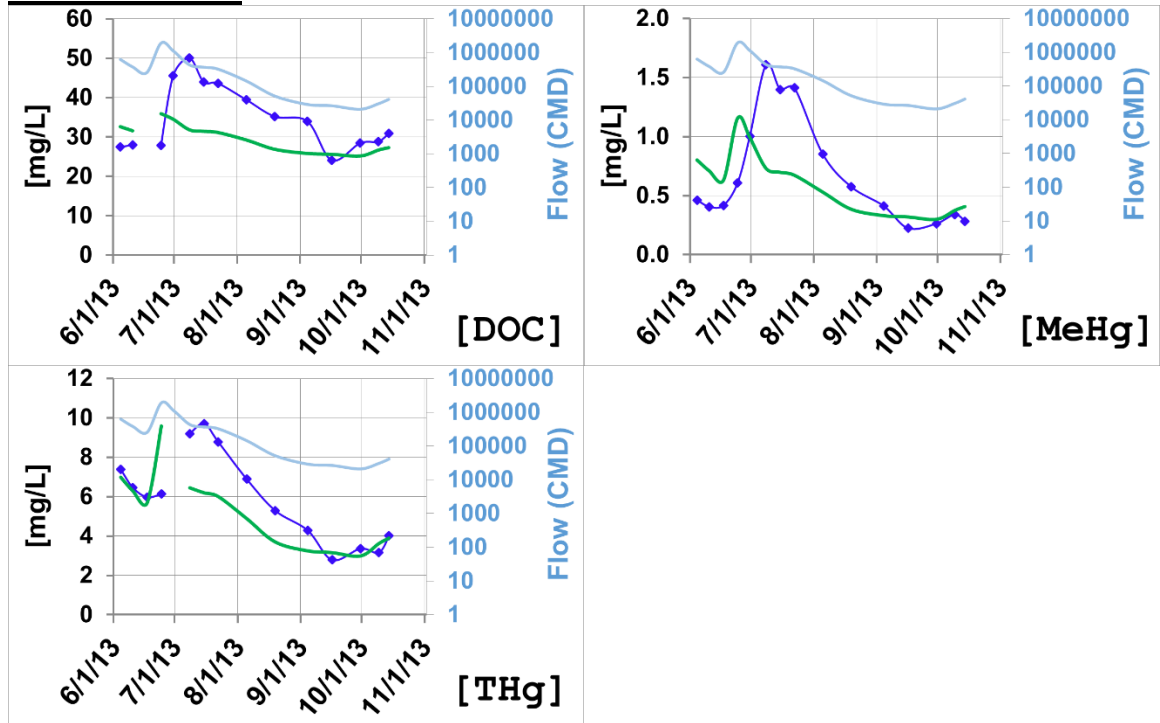


## Partridge River

### RIM RESULTS

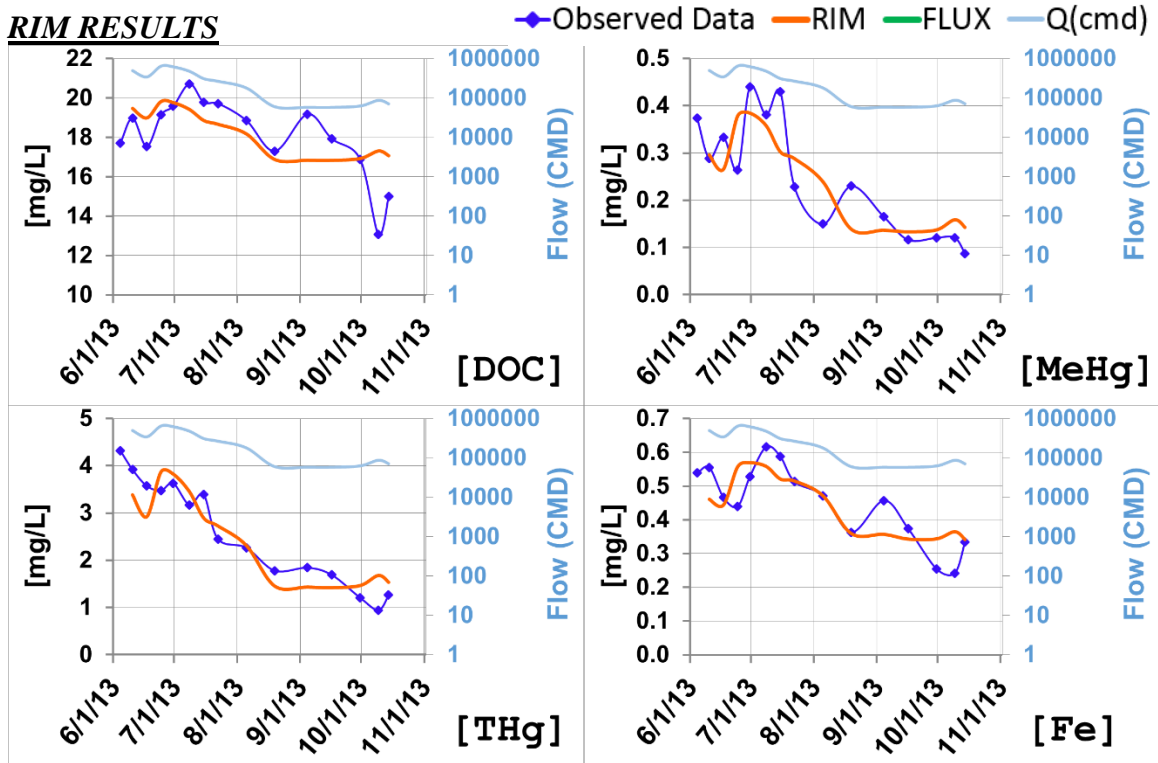


### FLUX RESULTS



## Embarrass River

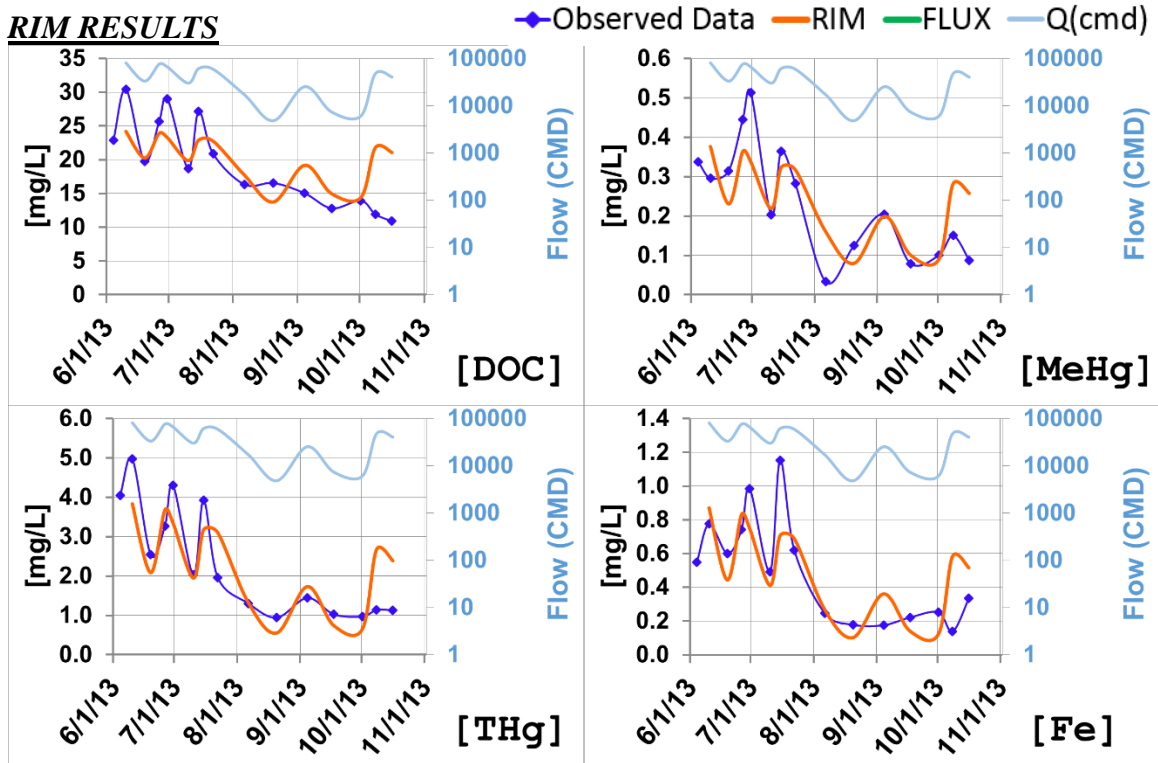
### RIM RESULTS



NO FLUX RESULTS AVAILABLE

## West Two River

### RIM RESULTS



NO FLUX RESULTS AVAILABLE

## **Appendix 2**

### RIM Parameters

SLR - MILE 179 : SKIBO		DOC [mg*L-1]	MeHg [ng*L-1]	Thg [ng*L-1]	Fe [mg*L-1]
$C_d =$		22.0	0.1	2.4	1.8
$MEAN C_0 =$		35.26	0.38	5.88	1.72
$d =$		0.17	0.17	0.17	0.17
$a =$		2935.90	2935.90	2935.90	2935.90
$b =$		17.01	17.01	17.01	17.01
$c_0 =$		21.91	0.08	1.60	0.02
$\Gamma_0 = (f/b) =$		0.00	0.08	0.14	0.00
$\eta = (b+f)/b =$		1.00	1.08	1.14	1.00
$f =$		0.023158973	1.291593593	2.426357121	0
$k =$		0	0	0	0.072034474
$\lambda =$		0.070134996	0.02237312	0.008322983	0.005775573
$n =$		26	26	26	26
$NS =$		0.726	0.796	0.798	0.519

SLR - MILE 94 : FORBES		DOC [mg*L-1]	MeHg [ng*L-1]	Thg [ng*L-1]	Fe [mg*L-1]
$C_d =$		17.0	0.1	2.0	0.5
$MEAN C_0 =$		25.33	0.43	4.26	0.96
$d =$		0.16	0.16	0.16	0.16
$a =$		135795.40	135795.40	135795.40	135795.40
$b =$		18.50	18.50	18.50	18.50
$c_0 =$		11.34	0.09	0.84	0.16
$\Gamma_0 = (f/b) =$		0.14	0.11	0.29	0.01
$\eta = (b+f)/b =$		1.14	1.11	1.29	1.01
$f =$		2.525797929	1.974758246	5.386924236	0.24133818
$k =$		0	0	0	0
$\lambda =$		0.007989937	0.023613618	0.005514121	0.061036236
$n =$		15	15	15	15
$NS =$		0.775	0.730	0.856	0.883

SLR - MILE 36		DOC [mg*L-1]	MeHg [ng*L-1]	Thg [ng*L-1]	Fe [mg*L-1]
$C_d =$		17.5	0.1	1.7	0.5
$MEAN C_0 =$		26.22	0.30	3.88	0.76
$d =$		0.15	0.15	0.15	0.15
$a =$		840636.07	840636.07	840636.07	840636.07
$b =$		20.98	20.98	20.98	20.98
$c_0 =$		14.80	0.07	0.98	0.21
$\Gamma_0 = (f/b) =$		0.05	0.09	0.18	0.01
$\eta = (b+f)/b =$		1.05	1.09	1.18	1.01
$f =$		1.130095625	1.917576712	3.853260262	0.14025088
$k =$		0	0.004303701	0.003127027	0
$\lambda =$		0.018845658	0.022082008	0.009245955	0.06539005
$n =$		27	27	27	27
$NS =$		0.586	0.466	0.732	0.598

WHITEFACE RIVER		DOC [mg*L-1]	MeHg [ng*L-1]	Thg [ng*L-1]	Fe [mg*L-1]
$C_d$ =		23.5	0.2	3.0	1.1
$MEAN C_0$ =		32.29	0.43	4.63	1.10
$d$ =		0.16	0.16	0.16	0.16
$a$ =		156580.50	156580.50	156580.50	156580.50
$b$ =		18.37	18.37	18.37	18.37
$c_0$ =		18.15	0.16	1.94	0.45
$\Gamma_0 = (f/b)$ =		0.09	0.14	0.15	0.01
$\eta = (b+f)/b$ =		1.09	1.14	1.15	1.01
$f$ =		1.615902548	2.647505942	2.777900775	0.271952315
$k$ =		0.001674182	0	0	0
$\lambda$ =		0.007238796	0.011791425	0.007994438	0.049253586
$n$ =		15	15	15	15
NS =		0.409	0.347	0.719	0.457

CLOQUET RIVER		DOC [mg*L-1]	MeHg [ng*L-1]	Thg [ng*L-1]	Fe [mg*L-1]
$C_d$ =		15.9	0.2	2.5	0.3
$MEAN C_0$ =		16.69	0.18	2.76	0.38
$d$ =		0.17	0.17	0.17	0.17
$a$ =		570173.10	570173.10	570173.10	570173.10
$b$ =		17.87	17.87	17.87	17.87
$c_0$ =		14.14	0.10	1.29	0.27
$\Gamma_0 = (f/b)$ =		0.04	0.12	0.22	0.02
$\eta = (b+f)/b$ =		1.04	1.12	1.22	1.02
$f$ =		0.691339679	2.231337684	3.948497627	0.389915345
$k$ =		0	0	0	0
$\lambda$ =		0.009198474	0.007114572	0.00344254	0.030420027
$n$ =		15	15	15	15
NS =		0.310	0.210	0.470	0.376

FLOODWOOD RIVER		DOC [mg*L-1]	MeHg [ng*L-1]	Thg [ng*L-1]	Fe [mg*L-1]
$C_d$ =		30.2	0.2	2.8	1.0
$MEAN C_0$ =		34.78	0.28	3.20	0.91
$d$ =		0.17	0.17	0.17	0.17
$a$ =		17174.90	17174.90	17174.90	17174.90
$b$ =		16.82	16.82	16.82	16.82
$c_0$ =		26.95	0.12	2.11	0.34
$\Gamma_0 = (f/b)$ =		0.04	0.17	0.10	0.00
$\eta = (b+f)/b$ =		1.04	1.17	1.10	1.00
$f$ =		0.670094888	2.900179823	1.614933711	0
$k$ =		0.001685369	0.000806108	0	0.018104598
$\lambda$ =		0	0	0	0.009392916
$n$ =		11	11	11	11
NS =		0.064	0.236	0.434	0.202

SWAN RIVER		DOC [mg*L-1]	MeHg [ng*L-1]	Thg [ng*L-1]	Fe [mg*L-1]
$C_d$ =		21.2	0.3	4.0	1.1
$MEAN C_0$ =		28.28	0.42	4.09	1.01
$d$ =		0.17	0.17	0.17	0.17
$a$ =		21921.30	21921.30	21921.30	21921.30
$b$ =		16.23	16.23	16.23	16.23
$c_0$ =		13.30	0.17	3.08	0.19
$\Gamma_0 = (f/b)$ =		0.17	0.20	0.09	0.10
$\eta = (b+f)/b$ =		1.17	1.20	1.09	1.10
$f$ =		2.73222243	3.298246454	1.520415349	1.636751993
$\kappa$ =		0.001372039	0.000829266	0	0.012610462
$\lambda$ =		1.50415E-06	0	0	0.016820521
$n$ =		15	15	15	15
NS =		0.485	0.193	0.350	0.241

PARTRIDGE RIVER		DOC [mg*L-1]	MeHg [ng*L-1]	Thg [ng*L-1]	Fe [mg*L-1]
$C_d$ =		28.4	0.3	3.4	1.7
$MEAN C_0$ =		34.81	0.68	5.96	1.90
$d$ =		0.16	0.16	0.16	0.16
$a$ =		20962.20	20962.20	20962.20	20962.20
$b$ =		17.31	17.31	17.31	17.31
$c_0$ =		28.42	0.26	2.94	0.06
$\Gamma_0 = (f/b)$ =		0.00	0.01	0.05	0.00
$\eta = (b+f)/b$ =		1.00	1.01	1.05	1.00
$f$ =		0.003624409	0.10664573	0.826885185	0.005328566
$\kappa$ =		0	0	0	0.051335806
$\lambda$ =		0.096433103	0.063960952	0.023745549	0.101301349
$n$ =		15	15	15	15
NS =		0.521	0.717	0.655	0.857

EMBARRASS RIVER		DOC [mg*L-1]	MeHg [ng*L-1]	Thg [ng*L-1]	Fe [mg*L-1]
$C_d$ =		17.9	0.1	1.7	0.4
$MEAN C_0$ =		18.09	0.25	2.59	0.45
$d$ =		0.17	0.17	0.17	0.17
$a$ =		57913.70	57913.70	57913.70	57913.70
$b$ =		16.16	16.16	16.16	16.16
$c_0$ =		14.89	0.05	0.53	0.09
$\Gamma_0 = (f/b)$ =		0.07	0.30	0.43	0.25
$\eta = (b+f)/b$ =		1.07	1.30	1.43	1.25
$f$ =		1.094432112	4.906391261	6.86934087	4.115398733
$\kappa$ =		0	0	0.002713958	0.014967043
$\lambda$ =		0	0.007969035	0	0
$n$ =		14	14	14	14
NS =		0.350	0.666	0.835	0.622

WEST TWO RIVER		DOC [mg*L-1]	MeHg [ng*L-1]	Thg [ng*L-1]	Fe [mg*L-1]
$C_d$ =		16.6	0.1	0.9	0.2
$^{MEAN}C_0$ =		19.46	0.24	2.33	0.50
$d$ =		0.19	0.19	0.19	0.19
$a$ =		4833.40	4833.40	4833.40	4833.40
$b$ =		13.93	13.93	13.93	13.93
$c_0$ =		9.73	0.03	0.15	0.02
$\Gamma_0 = (f/b)$ =		0.20	0.55	0.69	0.76
$\eta = (b+f)/b$ =		1.20	1.55	1.69	1.76
$f$ =		2.797407277	7.672442504	9.565441703	10.59471467
$\kappa$ =		0	0	0	0
$\lambda$ =		0	0	0	0
$n$ =		14	14	14	14
NS =		0.404	0.570	0.643	0.566